FMH606 Master's Thesis 2021
Process Technology

Mathematical models for the physicochemical properties of different amine-based solvents in post combustion capture

Jeanette Larsen

Faculty of Technology, Natural sciences and Maritime Sciences
Campus Porsgrunn

University of
South-Eastern Norway

Course: FMH606 Master's Thesis, 2021

Title: Mathematical models for the physicochemical properties of different amine-based solvents in post combustion capture

Number of pages: 81

Keywords: PCC, Aqueous amine solutions, CO_2 Capture, MATLAB, Aspen Plus

Student:	Jeanette Larsen
Main supervisor:	Sumudu Shanaka Karunarathne
Co-supervisor:	Lars Erik Øi

Summary:

CO_2 emissions caused by human activity is an increasing problem in today's society. In order to reduce the environmental impact, it is important to be able to design CO_2 capture modules from correct physicochemical properties. This includes accurately predicting the density and viscosity of pure, aqueous and CO_2 loaded aqueous amine solutions. The main objective of this thesis is therefore to explore mathematical correlations for physicochemical properties of different amine-based solvents applied to post combustion CO_2 capture.

13 developed correlations have been evaluated by comparing the maximum deviation of fitted models to the measured property, and by determining the average absolute relative deviation (AARD%). All calculations were performed by utilizing Python 3.6 and MATLAB R2020b. Post-processing of results were done in Excel.

The result of this thesis indicates that viscosity for aqueous amines are better correlated to Eyring's viscosity model based on the NRTL relation rather than with a Redlich-Kister correlation. This can be viewed by the achieved AARD% of aqueous MEA showing a value of 2.39 for Redlich-Kister, 1.87 for Eyring-NRTL and 1.88 for the segment-based Eyring-NRTL model. The same behavior was observed in calculations for aqueous MDEA. In addition, two correlations by Karunarathne et al. gave satisfactory results for CO_2 loaded aqueous MEA in the calculation of density and viscosity. The relations gave an AARD% of 0.15 and 0.53 respectively.

Lastly, it was found that by using an additional correlation from the research by Karunarathne et al., NRTL parameters from VLE data simulated in Aspen Plus may be used to estimate mixture viscosities.

Preface

This master thesis was written as my final assignment in the master program Process Technology at the University of South-Eastern Norway (USN). The project sparked my interest as it covers CO_2 capture technology, which is a field I would like to continue to explore in the future. During this project, I have gained a lot of knowledge on the amine absorption/ desorption process and associated solvents.

In the completion of my last year at USN, I would like to express gratitude to my supervisors, Sumudu S. Karunarathne, Associate professor at USN, and Lars Erik Øi, Head of department and Professor at USN. Their great guidance and suggestions have been essential in the completion of this thesis. They always believed in me and inspired me to continue working. In addition, I would also like to thank Finn Aakre Haugen, Professor at USN, for contributing with Python coding.

The idea of completing this master program started in 2016, where I failed at keeping up with the classes. At this time, I was unsure of whether I should try again in 2017. Then things changed, I got a new job which was relevant to my education and I gained friends at USN who were eager to discuss the different class subjects. This made it possible for me to continue the education. I will forever be grateful for all the help and great discussions I have had with my friends and colleagues.

Lastly, I would like to thank my partner. He has been my number one supporter throughout this project, cheering me on when I felt inadequate to complete the thesis. These 4 years of part-time studies combined with a full-time job would not have been manageable without encouragements from him.

Hammerfest, 30.09.21

Jeanette Larsen

Jeanette Larsen

Contents

Nomenclature

Symbols	Description	Units
α	Nonrandomness factor	
E	Empirical constant in Eyring's viscosity model	
ΔF^*	Free energy of activation for viscous flow	J/mol
ΔF^{E*}	Excess free energy of activation for viscous flow	J/mol
ΔF_{Eyring}^{E*}	Excess free energy of mixing for viscous flow, from Eyring's activation energy theory in liquid mixtures (see ΔF^{E*})	J/mol
ΔG^{E*}	Gibbs excess free energy of mixing - component based	J/mol
$\Delta \tilde{G}^{E*}$	Gibbs excess free energy of mixing – for segments of moles	J/mol
g	Interaction energy parameter in NRTL equation	
h	Planck's constant	J/Hz
$i,\ j,\ k̦$	Any component	
k, m, n	Group	
M	Molecular weight	kg/mol
$ɱ$	Molecules	
N	Total number of polymer and solvent moles	
N_A	Avogadro's number	mol^{-1}
N_s	Total number of polymer segment and solvent moles	
η	Viscosity	$mPa \cdot s$
ρ	Density	kg/m^3
q	Surface area parameter	
Q	Group surface area	
R	Universal gas constant	$J \cdot K^{-1}\, mol^{-1}$

R_k	Group volume	
r	Average number of segments	
s	Volume parameter	
T	Temperature	K
τ	Interaction energy between different species	
u	Interaction energy parameter in UNIQUAC equation	
V	Molar volume	m^3/mol
V^E	Excess molar volume	m^3/mol
w	Mass ratio	
x_i	Mole fraction of component	
$\overline{x_i}$	Segment of moles	
X_j	Mole fraction or mole fraction multiplied by electric charge (Z)	
γ	Residual group activity coefficient in UNIFAC equation	
Z	Charge number of ions	
z	Coordination number in UNIQUAC/UNIFAC equation	
θ	Surface area fraction	
ϕ	Volume fraction	
ψ	CO_2 loading (mol CO_2/mol MEA)	

Abbreviations

AARD	Average absolute relative deviation
AMD	Absolute maximum deviation
AMP	2-Amino-2-methyl-1-propanol
APV100	Aspen Plus Version 10.0
DMEA	N-Dimethylethanolamine
DEA	Diethanolamine
DEEA	N-Diethylethanolamine
IEA	International Energy Agency
MEA	Monoethanolamine
MDEA	N-Methyldiethanolamine
MRSD	Mean relative standard deviation
NIST	National Institute of Standards and Technology (U.S. Department of commerce)
NRTL	Non-random two liquid model
PCC	Post combustion (CO_2) capture
UNIQUAC	Universal quasichemical activity coefficient model
UNIFAC	UNIQUAC Functional-group activity coefficient model
VLE	Vapor-liquid equilibrium

1 Introduction

This master thesis was written in collaboration with the University of South-Eastern Norway (USN). The proceeding sub-chapters will detail the background and objective of the thesis.

1.1 Background

In today's society, it is necessary to explore methods to reduce climate change caused by a growing energy demand. The CO_2 emissions in the last 30 years has increased by 12.5 gigatonnes globally. This is shown in Figure 1.1, where the pandemic due to lockdowns only impacted 2 Gt from 2019 to 2020. The subsequent trend for 2021 shows that emission levels are back on the rise, where estimations for the end of the year point towards a peak at 1.2% below the 2019 numbers [1]. To slow global warming, measures must be taken to reduce the large amount of emissions.
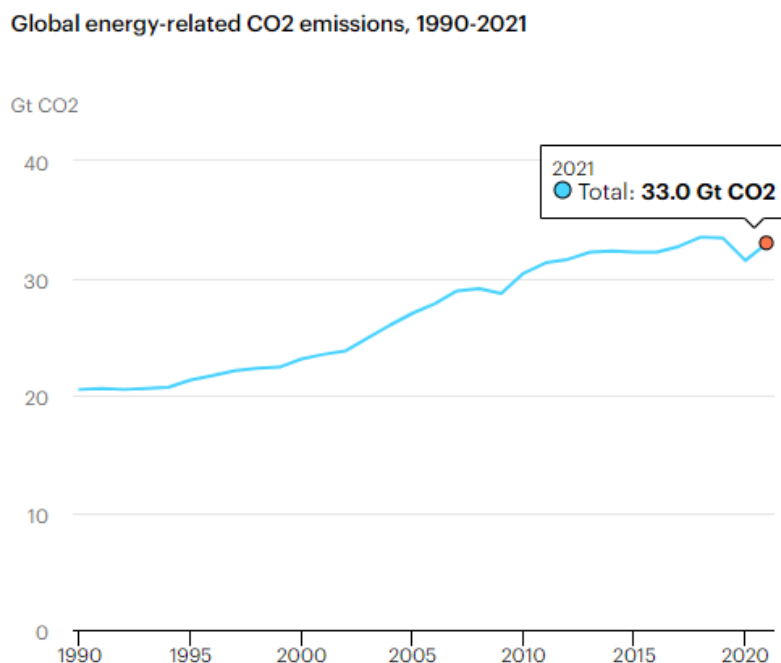
Figure 1.1: Reported CO_2 emissions from Global Energy Review by IEA [1].

The oil and gas industry use raw natural gas to operate turbines in order to generate electricity for liquefied natural gas or oil production. In this operation, a considerable amount of CO_2 is released from the combustion process into the atmosphere. This industry represents a quarter of the total CO_2 emissions in Norway [2].

A solution which is currently being explored is to transition platforms to operate by a low-carbon principle by laying electric cables from the mainland to replace the gas turbines [3]. The downside to this solution is that it requires new infrastructure in the form of transmission towers and power stations. Another solution to this problem would be to redesign gas turbines to operate with a post combustion CO_2 capture module. For these systems it is vital to be able to predict the physicochemical properties of amine-based solvents. The information can be

used to portray scenarios of post combustion capture to properly size equipment and ensure the desired efficiency of the system.

1.2 Outline of thesis

Chapter 2 explores amine-based solvents and how CO_2 capture is performed. The effect of the physicochemical properties is also included.

Chapter 3 shows a review of mathematical models of density and viscosity applied in literature for pure and liquid mixtures. The research also goes into depth of using different vapor-liquid equilibrium models for the Gibbs excess free energy to represent the nonideal term in Eyring's viscosity model.

Chapter 4 contains performed calculations and results which investigate existing and new mathematical correlations for density and viscosity. Pure and aqueous amines was curve fitted to empirical, semi-empirical and semi-theoretical models, while CO_2 loaded aqueous MEA density and viscosity were fitted to empirical models.

Chapter 6 discusses results obtained from curve fitting models. This includes an evaluation of applied models for pure amines and CO_2 loaded aqueous MEA. The discussion also compares empirical and semi-empirical models for the viscosity of aqueous MEA and aqueous MDEA.

Chapter 7 includes the conclusion of applied models and possible further work.

1.3 Abstract

The thesis explores post combustion CO_2 capture with amine solvents with the intent to gain a better understanding of these systems. This includes an in-depth review of theoretical, semi-empirical and empirical models of density and viscosity for pure and liquid mixtures. The information was used to develop correlations for density and viscosity of pure, aqueous and CO_2 loaded aqueous amine mixtures.

Further, the thesis includes discussions on developed correlations and the possibility of using vapor-liquid equilibrium models to represent viscosity. The applied models for calculations in this thesis include 13 correlations of varying complexity in which 3 models correlate to Eyring's viscosity model. This was performed to evaluate the best correlation for aqueous MEA and aqueous MDEA. The correlations included Eyring's model with a Redlich-Kister polynomial, Eyring-NRTL model and the segment-based Eyring NRTL model. The Eyring-NRTL model was computed with binary interaction parameters from VLE data simulated in Aspen Plus version 10.

2 Post combustion CO$_2$ capture

The following sub-chapters explains the necessity of amine-based solvents in CO$_2$ capture from flue gas, different amine types and how physicochemical properties affects the process.

2.1 CO$_2$ capture technology

The CO$_2$ capture in exhaust systems is performed at atmospheric pressure. Low CO$_2$ Partial pressure and low concentration in raw flue gas makes it more difficult to perform this operation in exhaust systems than in natural gas separation. The partial pressure ranges from 0.14 bar ($\approx$2psia) to treated flue gas at 0.018 bar ($\approx$0.26 psia) which favors CO$_2$ capture by amine-solvents [4]. Figure 2.1 shows the different methods for CO$_2$ removal depending on the partial pressure of the feed and product.
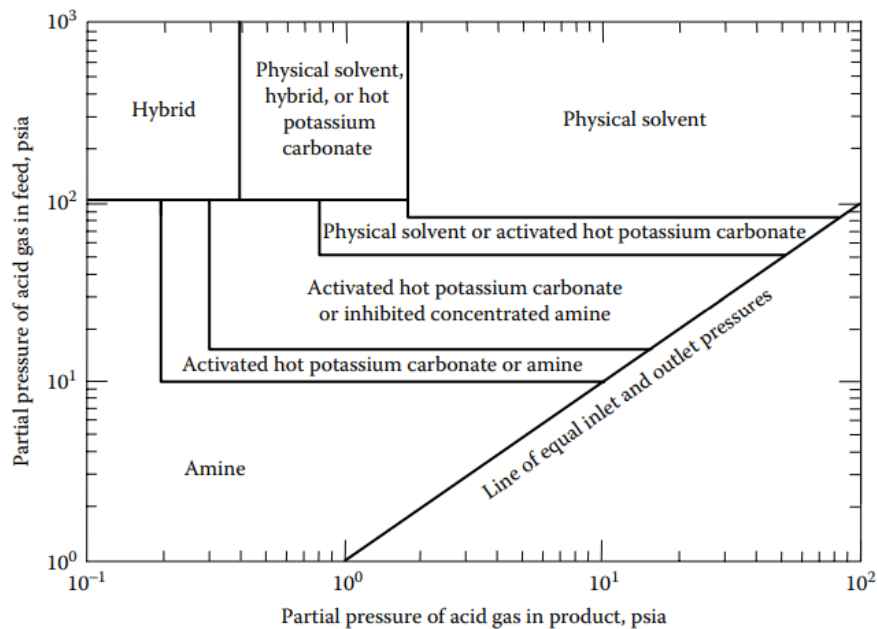

Figure 2.1 Overview of acid gas removal methods where "product" can be viewed as treated flue gas [5].

In post combustion capture (PCC), the flue gas from a gas turbine is sent through an absorption column. The gas is directed from the bottom inlet to the top outlet, and crosses paths with a liquid absorption solvent. In this case, the amine solvent reacts with the CO$_2$ and cleans the gas to be released to the atmosphere [5].

In the next step, the CO$_2$ rich amine continues to a stripper column, where the temperature is increased by a connected reboiler. The high temperature causes the amine to release CO$_2$ through the top of the column. This process is known as regeneration, where the lean amine can be reused in the absorption column. The outlet stream of CO$_2$ can now be cooled, pressurized and sent offshore to be stored in formations below the seabed [5].

An example of this process is shown in Figure 2.2. The illustration also shows that the process could be optimized by using rich amine to cool regenerated lean amine.
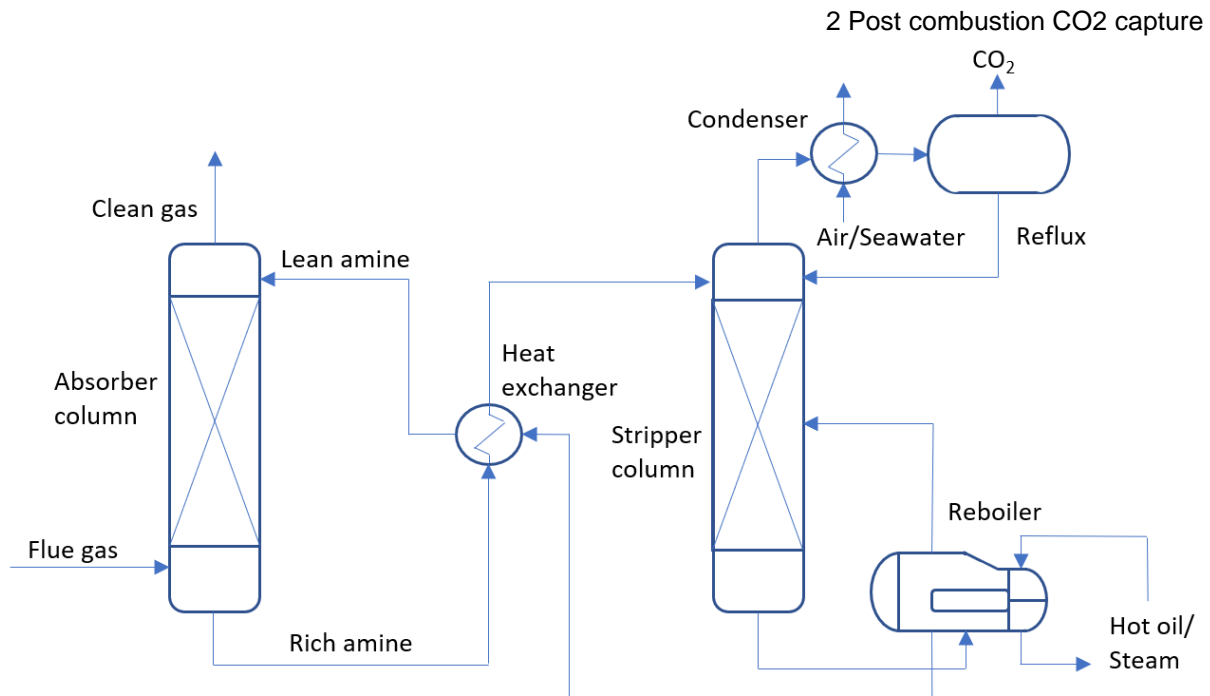
Figure 2.2 Simplified overview of CO_2 capture.

2.2 Amine solvents

Amines are bases which are produced by altering the hydrogen content of ammonia (NH_3). For primary amines this includes inserting a hydrocarbon molecule in the place of one of the hydrogen atoms. The same principle extends to secondary and tertiary amines, by substituting 2 or 3 atoms of hydrogen [5].

Monoethanolamine (MEA) is a primary amine and one of the most commonly used solvents in PCC. It has a high reaction rate with CO_2, and the thermal stability is reported to be good. Considering positive aspects of this solvent, the downside to using MEA is the low absorption capacity, high energy demand and high makeup rate. This occurs during the regeneration process where the temperature causes vaporization of MEA. High temperatures are required to break the stable formation of carbamates between CO_2 and MEA. Another widely used solvent is Diethanolamine (DEA), a secondary amine which can be operated with a lower heat of reaction. In comparison to MEA, this solvent absorbs CO_2 at a slower rate [6].

In order to create an optimized amine solvent, tertiary amines can be added to reduce unwanted characteristics of primary amines. This group has a high CO_2 loading capacity and consists of the solvents N-Methyldiethanolamine (MDEA), N-Dimethylethanolamine (DMEA) and N-Diethylethanolamine (DEEA). In detail, MDEA resists degradation better than primary and secondary amines, but shares a low absorption rate with DEA. DMEA on the other hand, at some temperature levels has been proven to exhibit better reaction rates than MDEA [7]. DEEA also has a faster reaction with CO_2 than MDEA and is considered to be the environmentally friendly capture solvent. The main part of DEEA consists of ethanol which can be extracted from agricultural waste [8].

Lastly, the group of sterically hindered amines is often represented by 2-amino-2-methyl-1-propanol (AMP). The solvent has a high CO_2 loading capacity due to forming unstable carbamates which allows for a higher reaction rate constant. [9]. All of the above-mentioned amines have been entered in Table 2.1 for comparison.

Table 2.1 Comparison of amine types from various research articles.

Amine group	Amine type	Fast reaction with CO_2	Slow reaction with CO_2	High CO_2 load Capacity	Resists Degradation/corrosion	Low regeneration energy	High makeup rate	Environmentally friendly
Primary	MEA	x [6]					x [6]	
Secondary	DEA		x [6]	x [6]		x [6]		
Tertiary	MDEA		x [6], [7]	x [7], [8]	x [7]	x [6], [7], [8]		
	DMEA		X [7] Faster than MDEA	x [7]	x [7]	x [7]		
	DEEA		X [8] Faster than MDEA	x [8]				x [8]
Sterically hindered	AMP		X [9] Faster than MDEA	x [9]		x [9]		

2.3 Importance of viscosity and density in PCC

Viscosity is viewed as the key property of CO_2 post combustion capture. This is described in research by Conway et al. where an increase in viscosity affects the mass transfer of CO_2 to the liquid amine. This is mentioned as a possible setback when using amine concentrations larger than 30 wt% with the intent of increasing CO_2 absorption rates [10]. The importance of viscosity is also supported by Di Song et al. Their work states that a high viscosity can affect loaded amine returning to the amine solution by slowing this diffusion process as well. Additionally, it was reported that this could cause lower liquid turbulence on the surface of the structured packing inside absorption/desorption columns [11].

Nookuea performed research on density correlations, which concluded that an 11% difference in calculations would impact the packing height of the absorber. The same research clarified that CO_2 removal rates and CO_2 loading were less affected by density than viscosity [12].

3 Literature review

This chapter displays the research literature for the theoretical, semi-empirical and empirical models of density and viscosity for pure and liquid mixtures. The study was also focused on viscosity models in process simulation tools, as one of the main discussion points of this thesis revolves around using vapor-liquid equilibrium models to estimate viscosity. For CO_2 capture, there are many process simulation tools such as UniSim, Aspen Hysys and CHEMCAD. However, most of the reviewed literature in this thesis include the application of Aspen Plus. Thus, the review was limited to comparing available models in Aspen Plus Version 10 (APV100) to correlations found in literature. The proceeding sub-chapters also contain information about the average absolute relative deviation (AARD%) which is elaborated in Chapter 4.

3.1 Density of pure liquids

The measured density of a liquid can be curve fitted and correlated through a polynomial as shown in Eq (3.1). The empirical method was presented in research by Al-Ghawas et al. for MDEA [13]. The research included the equation as it conveniently displayed good agreement to density data. Al-Ghawas et al. reported that the equation was able to predict experimental data with an average mean deviation of 0.05%. The research included aqueous MDEA, but the formula does not consider the mole fraction of different components. Thus, parameters were changed for each mole fraction of MDEA.

$$\rho = A + BT + CT^2 \tag{3.1}$$

3.2 Viscosity of pure liquids

The Andrade Eq (3.2) in its Arrhenius form is often used in articles to portray the viscosity of pure liquids. The model has parameters that is decided empirically through curve fitting and is therefore considered semi-theoretical. The equation relates temperature to viscosity by B which contains the activation energy and Boltzmann constant ($-E/k$), while A represents molecular weight and density ($M^{\frac{3}{2}}\rho^{-\frac{1}{3}}$). Andrade proved that his formula was able to obtain the viscosity of water with a deviation of 0.5 percent in a temperature range from 60°C to 100°C [14].

$$n = Ae^{\frac{B}{T}} \iff \ln(n) = \ln(A) + \left(\frac{B}{T}\right) \tag{3.2}$$

Since the 1930's, many versions of this equation have been created. This can be seen in Aspen Plus where the Andrade Eq (3.3) has been adapted with an extra parameter C.

$$\ln \eta = A_i + \frac{B_i}{T} + C_i \ln T \tag{3.3}$$

In Aspen Plus all parameters are retrieved from various sources both from research literature and different data banks.

3.3 Density of liquid mixtures

The density of liquid mixtures can be correlated through Eq (3.4) by Aronu, Hartono and Svendsen [15]. The formula correlates mixtures but can be applied to pure liquids when the mole fraction of amine (x_1) is set equal to 1 and the other substance is excluded ($x_2 = 0$). The experiments of Aronu et al. included the density of concentrated and amine-based aqueous amino acid salt solutions. The research gave satisfactory results with an AARD% of 0.19 for the concentrated solution and 0.14 for the amine-based solution.

$$\rho = \left(k_1 + \frac{k_2 x_2}{T}\right) \exp\left(\frac{k_3}{T^2} + \frac{k_4 x_1}{T} + k_5 \left(\frac{x_1}{T}\right)^2\right) \tag{3.4}$$

Another method was used by Hartono, Mba and Svendsen. This included using a simplified Redlich-Kister model by correlating density in Eq (3.5) to the excess molar volume (V^E) by Eq (3.6). The procedure was reported by Hartono et al. to show an even better fit than the Aronu et al. correlation with an AARD% at 0.04 for aqueous MEA [16].

$$\rho = \frac{\left(\sum_1^2 x_i \cdot M_i\right)}{V^E + \left(\sum_1^2 x_i \cdot \frac{M_i}{\rho_i}\right)} \tag{3.5}$$

$$V^E = (k_1 + k_2 T + k_3 x_1 + k_4 x_1^2) \cdot x_1 x_2 \tag{3.6}$$

Hartono et al. also investigated CO_2 loaded solutions with the creation of Eq (3.7). The research relates volume expansion (Φ) by Eq (3.8) to the CO_2 addition per kg of the aqueous mixture by Eq (3.9). This is based on their findings that marginally higher densities were observed when only the weight of CO_2 was considered. The evaluation gave an AARD% 0.04 and 0.13 for the mass ratio of 0.062 and 0.3 between MEA and water. Calculations included a CO_2 loading in the range of 0 to 0.5. For these equations the notation for CO_2 loading was changed from α in the work of Hartono et al. to ψ in this thesis [16].

$$\rho_{CO_2 \, loaded} = \frac{\rho_{loaded}}{1 - w_{CO_2 \, added} \cdot (1 - \Phi^3)} \tag{3.7}$$

$$\Phi = \frac{a_1 x_1 \psi + a_2 x_1}{a_3 + x_1} \tag{3.8}$$

$$\frac{w_{CO_2 \, added}}{kg_{CO_2 \, added} \cdot kg_{solution}^{-1}} = \frac{\psi x_1 M_3}{x_1 M_2 + (1 - x_1 - \psi x_1) M_2 + \psi x_1 M_3} \tag{3.9}$$

CO_2 loaded amine mixtures were also explored by Karunarathne et al., where Eq (3.4) was extended into Eq (3.10) to cover density of CO_2 loaded aqueous MEA. The formula evaluates different CO_2 loadings at specific mole fractions of MEA achieving an AARD% of 0.08% and 0.15% at mass ratios 0.3 and 0.4 [17].

$$\rho = (a_1 + a_2(T) + a_3(T^2) + a_4 x_3)\left(k_1 + \frac{k_2 x_2}{T}\right) \exp\left(\frac{k_3}{T} + \frac{k_4 x_1}{T} + k_5 \left(\frac{x_1}{T}\right)^2\right) \tag{3.10}$$

3.4 Viscosity of liquid mixtures

The viscosity of aqueous mixtures can be correlated through Eq (3.11) by considering a viscosity deviation (η_d). This method is based on the difference between the ideal viscosity (η) and the sum of individual component viscosities (η_i). The procedure was used by Hartono et al., and is similar to the formula mentioned for density in Chapter 3.3. In the research, they correlated the viscosity deviation to a simplified Redlich-Kister model as shown by Eq (3.12) [16]. The calculations by Hartono et al. obtained an AARD% of 4.2 for aqueous MEA.

$$\ln(\eta) = \ln(\eta_d) + \sum_{1}^{2} x_i \ln(\eta_i) \tag{3.11}$$

$$\ln(\eta_d) = (l_1 + l_2 T + l_3 T^2 + l_4 x_1) x_1 x_2 \tag{3.12}$$

To achieve an even better fit for the AARD%, the viscosity of aqueous mixtures can be correlated through Eyring's viscosity model. In 1936, Henry Eyring and his colleagues studied rate-based processes in liquids which led to the development of Eq (3.13) [18]. The model parameters included Avogadro's number (N_A), Planck's constant (h), molar volume (V), free energy of activation (ΔF^*), gas constant (R) and temperature (T).

$$\eta = \frac{N_A h}{V} exp\left(\frac{\Delta F^*}{RT}\right) \tag{3.13}$$

The theory behind Eyring's viscosity model is based on chemical reactions where reactants leap across an energy barrier to reach the final state. The same thoughts were applicable when a shearing force creates continuous steady flow in a pure liquid. In this process, one molecule requires activation energy to move from its original placement to a neighboring vacant hole in the fluid [18].

Eyring's research further included mixtures by Eq (3.14) and (3.15), where the solvent was evaluated to affect the solution by contributing with holes for the solute [18]. Novak describes Eyring's equations as containing an "ideal part" from two components in a liquid by the free energy of activation (ΔF^*) and a "non ideal part" contributed by the excess free energy of mixing for viscous flow (ΔF_{Eyring}^{E*}) [19].

$$\eta = \frac{N_A h}{V} exp\left(x_1 \Delta F_1^* + x_2 \Delta F_2^* - \frac{\Delta F_{Eyring}^{E*}}{E}\right) / RT \tag{3.14}$$

$$\ln(\eta) = x_1 \ln(\eta_1) + x_2 \ln(\eta_2) \tag{3.15}$$

The combination of Eq (3.14) and Eq (3.15), with the constant $E = 1$ creates Eq (3.16) [19].

$$\ln(\eta V) = \sum_{i=1}^{i=2} x_i \ln(\eta_i V_i) - \frac{\Delta F_{Eyring}^{E*}}{RT} \tag{3.16}$$

According to Novak et al. it is also important to note that Eq (3.16) is not thermodynamically correct for an excess property [20] . The definition states that the excess value is the surplus when comparing the actual to the ideal solution for the same composition, temperature and

pressure. In other words, the equation would show the ideal free energy plus the excess value [21]. This could explain why the excess free energy of mixing for viscous flow is often changed by researchers to a positive integer ($+\Delta F_{Eyring}^{E*}$). To avoid confusion later in this thesis, the excess free energy of mixing (ΔF_{Eyring}^{E*}) contributed by viscous flow, will from now be referred to as the excess free energy of activation for viscous flow (ΔF^{E*}).

Creating a correlation directly for the excess free energy of activation was done by Karunarathne et al. through a Redlich-Kister polynomial. The research combined Eq (3.17) and (3.18), which gave an AARD% of 1.4 and an AMD of 0.79 for the viscosity of aqueous MEA [17].

$$\frac{\Delta F^{E*}}{RT} = x_1 x_2 \sum_{i=1}^{i=2} C_i (1 - 2x_2)^i \tag{3.17}$$

$$C_i = a_i + b_i(T) \tag{3.18}$$

Karunarathne et al. also investigated the viscosity of CO_2 loaded aqueous MEA. The work resulted in Eq (3.19) where properties of the unloaded mixture was applied to estimate the viscosity of the CO_2 loaded solution. The correlation was further used to evaluate Gibbs excess free energy of the CO_2 loaded case. For the viscosity of CO_2 loaded aqueous MEA, Karunarathne et al. achieved an AARD of 0.58% and 1.13% at an MEA mass ratio of 0.3 and 0.4 [17].

$$\ln(V\eta)_{CO_2\ loaded} - \ln(V\eta)_{unloaded} = x_3(d_1 + d_2 T + d_3 x_3) \tag{3.19}$$

By the concept of a density deviation (η_d), Hartono et al. also applied this method to CO_2 loaded aqueous MEA. The correlation in Eq (3.20) and (3.21) was used for a mass ratio of 0.3 which resulted in an AARD of 2%. The model was listed with its estimated parameters [16].

$$\ln(\eta)_{CO_2\ loaded} = x_3 \ln(\eta_d) + (1 - x_3)\ln(\eta)_{unloaded} \tag{3.20}$$

$$\ln(\eta_d) = \frac{(6.98 \pm 0.48) \cdot x_1 + (10.48 \pm 1.0)\psi x_1}{(0.049 \pm 0.008) + x_1} \tag{3.21}$$

3.4.1 Vapor-liquid equilibrium models

In later years, Eyring's viscosity model has been connected to VLE models in order to estimate the viscosity. This includes replacing the excess free energy of activation (ΔF^{E*}) by Gibbs excess free energy of mixing (ΔG^{E*}) [20]- [22]. In simple terms, Gibbs free energy is linked to chemical potential. A negative value for Gibbs free energy is referred to as spontaneous, meaning that a reaction will occur without additional energy from the surroundings [23].

3.4.1.1 Eyring-UNIQUAC

The concept of using the Universal quasichemical activity coefficient (UNIQUAC) model to represent the non-ideal term in Eyring's Eq (3.16) was tested by Wu in 1986. The calculation was performed on 13 ternary systems and was perceived to show good results [24]. Unfortunately, the research does not show applied equations, hence the UNIQUAC model was

retrieved from another source referencing the original equations by Abrams and Prausnitz [21]. Assumptions were made that Wu applied the UNIQUAC model as given by Eq (3.22) where Gibbs excess free energy is split into two terms referred to as the combinatorial (3.23) and residual term (3.24) [21]. The model variables include molecule properties like surface area parameter (q_i), surface area fraction (θ_i), volume fraction (ϕ_i), molar volume (V_i) and a coordination number (z) which is usually assigned the value of 10. Lastly, the interaction parameter between components (τ_{ji}) are given by Eq (3.25).

$$\frac{\Delta G^{E*}}{RT} = \left(\frac{\Delta G^{E*}}{RT}\right)_{comb} + \left(\frac{\Delta G^{E*}}{RT}\right)_{res} \tag{3.22}$$

$$\left(\frac{\Delta G^{E*}}{RT}\right)_{comb} = \sum_{i=1}^{n} x_i \ln\left(\frac{\phi_i}{x_i}\right) + \frac{z}{2}\sum_{i=1}^{n} q_i x_i \ln\left(\frac{\theta_i}{\phi_i}\right) \tag{3.23}$$

$$\left(\frac{\Delta G^{E*}}{RT}\right)_{res} = -\sum_{i=1}^{n} x_i q_i \ln\left(\sum_{j=1}^{n} \theta_j \tau_{ji}\right) \tag{3.24}$$

$$\tau_{ji} = exp\frac{-(u_{ji} - u_{ii})}{RT} \tag{3.25}$$

In 2000, Martins et al. took the research further and created a new correlation based on the same theory with a small modification to the formula. The research included testing different correlations for the ideal term in Eyring's model which resulted in the choice of Eq (3.26).

$$\ln\eta_{ideal} = \sum_{i=1}^{n} x_i \ln\eta_i \tag{3.26}$$

The trial and error method led to a combination of Eq (3.16), (3.22) and (3.26) which gave the "modified" Eyring-UNIQUAC model in Eq (3.27). In this thesis, the interaction parameter was changed from (ψ_{ki}) in Martins et al. research to (τ_{ji}) to conform with the notation given in Eq (3.24) [25].

$$\ln(\eta V) = \sum_{i=1}^{n} x_i \ln(\eta_i) + \ln\left(\sum_{i=1}^{n} x_i V_i\right)$$
$$+ \sum_{i=1}^{n} x_i \ln\left(\frac{\phi_i}{\theta_i}\right) + \frac{z}{2}\sum_{i=1}^{n} q_i x_i \ln\left(\frac{\theta_i}{\phi_i}\right) - \sum_{i=1}^{n} x_i q_i \ln\left(\sum_{j=1}^{n} \theta_i \tau_{ji}\right) \tag{3.27}$$

In Martins.et al research, the surface area fraction (θ_i) and volume fraction (ϕ_i) is given by Eq (3.28) and (3.29). The parameters in these equations (q_i, s_i) could be found by regressing experimental viscosity data or by using van der Waals surface area and group volume estimation [26].

$$\theta_i = \frac{x_i q_i}{\sum_{j=1}^{n} x_j q_j} \tag{3.28}$$

$$\phi_i = \frac{x_i s_i}{\sum_{j=1}^{n} x_j s_j} \tag{3.29}$$

The volume parameter in Eq (3.29) has been changed from (r_i) in the original source to (s_i) in this thesis to distinguish variables that share the same letter [26].

The research of Martins et al. included testing 352 binary systems at 1 bar and was found to achieve an overall mean relative standard deviation (MRSD) of 1.2% for these liquids. For systems containing water the MRSD was adjusted to 2.24% [25]. Martins et al. later used Eq (3.27) in calculating the viscosity for ternary and quaternary liquid mixtures. The test was performed on 48 ternary and 3 quaternary systems, where an overall MRSD was determined to be 2.95%. In these calculations, water systems reflected an MRSD of 4.88% [22].

Aspen plus V10 does not contain the Eyring-UNIQUAC model, but the UNIQUAC model is listed in terms of the liquid activity coefficients. This creates a possibility to apply the Method of UNIQUAC in determining the interaction parameters of the Eyring-UNIQUAC model by using Eq (3.30).

$$\tau_{ij} = \exp(a_{ij} + b_{ij}/T + c_{ij} lnT + d_{ij}T + e_{ij}/T^2) \tag{3.30}$$

3.4.1.2 UNIFAC-VISCO

From the research of Wu covering the UNIQUAC Equation, the main part consisted of exploring the UNIQUAC Functional-group Activity Coefficient (UNIFAC) model. Wu describes UNIFAC as a group contribution method which only requires pure component data. This creates a possibility to determine the viscosity of liquids when no experimental data is available. The model was correlated to Eyring's Eq (3.16), but again the equations are not clearly stated in his research. Instead, Wu made references to the UNIFAC equations for activity coefficients as created by Fredenslund, Jones and Prausnitz [24].

In 1988 Chevalier et al. proposed a similar viscosity correlation which has become known as the UNIFAC-VISCO model. The research contains a detailed overview showing Eq (3.31) based on Eyring's viscosity theory which includes the combinatorial term of UNIQUAC in Eq (3.23). For the residual term, Eq (3.32) uses the UNIFAC equation with the addition of a minus sign [27]. The interesting part of this relation is that Chevalier et al. uses the molecular weight (M) instead of the molar volume (V), which excludes the need to calculate the density of the mixture.

$$\ln(\eta M) = \sum^{i} x_i \ln(\eta_i M_i) + \left(\frac{\Delta G^{E*}}{RT}\right)_{comb} + \left(\frac{\Delta G^{E*}}{RT}\right)_{res} \tag{3.31}$$

$$\left(\frac{\Delta G^{E*}}{RT}\right)_{res} = -\sum^{i} x_i \ln \gamma_i^{*R} \tag{3.32}$$

In the UNIFAC-VISCO combinatorial term, Van der Waals' surface area and group volume are given by group constants (R_k, Q_k) in Eq (3.33). The values for the group constants can be found in research by Chevalier et al. [28].

$$s_i = \sum_{}^{k} n_k(i)R_k; \qquad q_i = \sum_{}^{k} n_k(i)Q_k \qquad (3.33)$$

And in the residual term, parameters are calculated by Eq (3.34) - (3.39) [27]. The original notation of interaction parameters (ψ_{nm}^*) was changed to (τ_{nm}) to align with notation in Aspen plus. In Eq (3.34) the term ($ln\,\gamma_k^*$) represents the residual group activity coefficient, while ($\ln \gamma_k^{*(i)}$) is the residual activity coefficient of group k in a reference solution composed of one type of molecules (i) . Therefore, Eq (3.35) is also used to calculate ($\ln \gamma_k^{*(i)}$) [28].

$$\ln \gamma_i^{*R} = \sum_{}^{k} n_k^{(i)}[\ln \gamma_k^* - \ln \gamma_k^{*(i)}] \qquad (3.34)$$

$$ln\,\gamma_k^* = Q_k \left[1 - \ln\left(\sum_{}^{m} \theta_m \tau_{mk} \right) - \sum_{}^{m} \frac{\theta_m \tau_{km}}{\sum^n \theta_n \tau_{nm}} \right] \qquad (3.35)$$

$$\theta_m = \frac{Q_m X_m}{\sum^n Q_n X_n} \qquad (3.36)$$

$$X_m = \frac{\sum^j n_m^{(j)} X_j}{\sum^j \sum^n n_n^{(j)} X_j} \qquad (3.37)$$

In Aspen plus the interaction parameters for the UNIFAC equation is related to temperature by Eq (3.38) and (3.39). In comparison, Chevalier et al. appears to only apply Eq (3.38) in the UNIFAC-VISCO model. From this relation, b_{nm} (shown as α_{nm} in the original work) can be determined through parameter tables included in their research [27].

$$\tau_{nm} = \exp\left(-\frac{b_{nm}}{T} \right) \qquad (3.38)$$

$$\tau_{nm} = exp - \left(\frac{a_{nm}}{T} + b_{nm} + c_{nm}T \right) \qquad (3.39)$$

The work of Chevalier et al. mainly covers the development of new interaction parameters for binary systems containing methanol and/or alcohol [27]. Further recommendations for the use of the model was given by Poling et al. This included recommendations to use the UNIFAC-VISCO for mixtures with component molecules varying greatly in size and when group interaction parameters were possible to obtain. But for systems containing water it was advised not to apply the method [26].

3.4.1.3 Eyring-NRTL

Another well-known way to represent Gibbs excess free energy is through the Non-random two liquid (NRTL) model. This was applied by Novak in creating the Eyring-NRTL model by combining Eq (3.16) and (3.40). In this relation, the nonrandomness (α) is given through Eq (3.41) and the interaction energy (τ) between molecules is represented by Eq (3.42). Novak kept the original minus sign for the excess free energy when setting up the correlation [19].

$$\frac{\Delta G^{E*}}{RT} = x_1 x_2 \left(\frac{G_{21}\,\tau_{21}}{x_1 + x_2 G_{21}} + \frac{G_{12}\tau_{12}}{x_1 G_{12} + x_2} \right)$$ (3.40)

$$G_{ij} = \exp\left(-\alpha_{ij} \cdot \tau_{ij}\right)$$ (3.41)

$$\tau_{ij} = (g_{ij} - g_{ji})/RT$$ (3.42)

Novak's research included a selection of pseudo binary systems, meaning that the components are mixtures rather than pure elements. The work concluded with a viscosity deviation of 0.2% [19]. The research results also implied that polymers (large molecules) flow in segments rather than a complete unit into a vacant hole as explained by Eyring's theory. Thus, Novak et al. also created the segment-based Eyring-NRTL model [20].

The Eyring-NRTL model was tested by karunarathne.et al in a research article covering MEA + H_2O and AMP + MEA + H_2O [29]. The work included binary interaction parameters from the article by Schmidt et al. which shows use of the NRTL equation with VLE data [30]. In the work of Karunarathne et al., the excess free energy of activation (ΔF^{E*}) was considered a positive value. Their calculations resulted in an additional correlation to the Gibbs excess free energy (ΔG^{E*}) of aqueous MEA in Eq (3.43). The relation gave an AARD% of 1.3 and an AMD of 1.

$$-\frac{\Delta G^{E*}}{\Delta F^{E*}} = a + bx_1 T + cT^2$$ (3.43)

The Eyring-NRTL model is referred in the help guide of Aspen Plus. The software describes Eq (3.44) to (3.45) which relates the temperature-dependent parameters, a through f, to Gibbs excess free energy (ΔG^{E*}).

$$\tau_{ij} = a_{ij} + \frac{b_{ij}}{T} + e_{ij} \ln T + f_{ij} T$$ (3.44)

$$\alpha_{ij} = c_{ij} + d_{ij}(T - 273.15K)$$ (3.45)

3.4.1.4 Electrolyte-NRTL

In 2013, Matins et al. replaced the excess term in Eyring's viscosity model from Eq (3.16) with the Gibbs free energy of mixing (ΔG_{mix}) by applying the Electrolyte-NRTL model. The excess term was tested both as positive and negative based on results from Novak's research for the Eyring-NRTL model. Results indicated that a positive term predicted a viscosity 4-5 times lower than the experimental data, while the negative expression ensured the most accurate

results. The choice of prefix for the free energy of mixing was therefore set as negative in Eq (3.46). The model was used to portray viscosity of CO_2 loaded aqueous MEA, where the two first terms on the right-hand side were limited to MEA and water due to lack of viscosity data for ions. Calculations by Eq (3.46) involved 3 different concentrations of aqueous MEA in the range of 313.15 to 343.15K with a CO_2 loading of 0.1 to 0.5 mol CO_2/mol MEA [31].

$$\ln(nV) = \sum_i x_i \ln(\eta_i) + \ln\left(\sum_i x_i V_i\right) - \frac{\Delta G_{mix}}{RT} \tag{3.46}$$

The Gibbs free energy of mixing in Matins et al. model is given by the summation of the ideal free energy and excess free energy of the mixture in Eq (3.47) [31]. References in the research implies that the ideal free energy of CO_2, MEA and water were calculated by Eq (3.48) [21].

$$\Delta G_{mix} = \Delta G_{id,mix} + \Delta G^{E*} \tag{3.47}$$

$$\Delta G_{id,mix} = \sum_i x_i G_i + RT \sum_i x_i \ln(x_i) \tag{3.48}$$

Matins research further included the NRTL part of the Electrolyte-NRTL equations by Chen et al. to represent Gibbs excess free energy in Eq (3.47). The model describes local electroneutrality where the first term contains molecules (ɱ) at the center where the electric charge (Z_j) of nearby anions (a, a') and cations (c, c') equate to zero [32]. In the second term cations are at the center surrounded by molecules and anions. The third term represents the inverse of the second term where anions are centered. Subscript j and ꝁ represent any species [33].

$$\frac{\Delta G^{E*}}{RT} = \sum_{ɱ} X_{ɱ} \frac{\sum_j X_j G_{iɱ} \tau_{iɱ}}{\sum_ꝁ X_ꝁ G_{kɱ}} + \sum_c X_c \sum_{a'} \frac{X_{a'} \sum_j G_{jc,a'c} \tau_{jc,a'c}}{(\sum_{a''} X_{a''})(\sum_ꝁ X_ꝁ G_{ꝁc,a'c})}$$
$$+ \sum_a X_a \sum_{c'} \frac{x_{c'} \sum_j G_{ja,c'a} \tau_{ja,c'a}}{(\sum_{c''} X_{c''})(\sum_ꝁ X_ꝁ G_{ꝁa,c'a})} \tag{3.49}$$

In Eq (3.49) $X_j = x_j C_j$ where $C_j = Z_j$ for anions and cations, while $C_j = 1$ for molecules to represent molfraction. Matins et al. used interaction parameters (τ) and nonrandomness parameters (α) estimated through Aspen Plus for CO_2, MEA, H_2O and associated ions (created in reactions) by Eq (3.49), (3.51), (3.52) and (3.53) [31].

$$G_{cm} = \frac{\sum_a X_a G_{ca,ɱ}}{\sum_{a'} X_{a'}} \tag{3.50}$$

$$\alpha_{cm} = \frac{\sum_a X_a \alpha_{ca,ɱ}}{\sum_{a'} X_{a'}} \tag{3.51}$$

$$G_{jc,a'c} = \exp\left(-\alpha_{jc,a'c}\,\tau_{jc,a'c}\right) \tag{3.52}$$

$$\tau_{\mathfrak{m}a,ca} = \tau_{am} - \tau_{ca,\mathfrak{m}} + \tau_{\mathfrak{m},ca} \tag{3.53}$$

From the above mentioned equations, the electrolyte-NRTL equation also covers $G_{a\mathfrak{m}}$ which is calculated by the form of Eq (3.50), while $G_{ja,c'a}, G_{ca,\mathfrak{m}}, G_{i\mathfrak{m}}$, is given by the form of Eq (3.52). The last interaction parameter $\tau_{\mathfrak{m}c,ac}$ is found by the configuration of Eq (3.53) by estimating terms $\tau_{c\mathfrak{m}}, \tau_{ca,\mathfrak{m}}$ and $\tau_{\mathfrak{m},ca}$ [32]. In equation (3.49) to (3.53), the original notation for molecules, m, and the letter for any species, k, was modified to avoid confusion with applied terms in the UNIQUAC model.

In Aspen Plus, the electrolyte-NRTL model is referred to as either symmetric or asymmetric, where the symmetric version for a nonaqueous solution can be reduced to the original NRTL equation. The software lists molecule-molecule pairs by Eq (3.44) and (3.45), while molecule-electrolyte and electrolyte-electrolyte pairs are given by the arrangement of Eq (3.54) with $T_{ref} = 298.15K$.

$$\tau_{m,ca} = C_{m,ca} - \frac{D_{m,ca}}{T} + E_{m,ca}\left[\frac{T_{ref} - T}{T} + \ln\left(\frac{T}{T_{ref}}\right)\right] \tag{3.54}$$

3.4.2 Relation independent of temperature

A new interesting equation to approximately determine the viscosity of binary and ternary liquids from pure component properties has been proposed by Bhatt in Eq (3.55). The method was tested for 3 binary and 2 ternary systems at a constant temperature of 298.15K. Bhatt tested the relation in comparison to Flory's statistical theory, which showed quite promising results [34]. The model is based on rheochor $(V_i \eta_i^{1/8})$ which is explained as a constant property used to compare the molar volumes of different liquids from the boiling point and downwards. The rheochor relation was developed by Newton Friend [35].

$$\eta = \left[\frac{\sum\left(x_i V_i \eta_i^{\frac{1}{8}}\right)}{\sum(x_i V_i)}\right]^8 \tag{3.55}$$

3.5 Problem description

Physicochemical properties are important in amine-based CO_2 capture processes, and through the literature search it has been shown that a wide variety of correlations exists. The aim of this thesis will therefore be to develop semi empirical and empirical correlations for density and viscosity of both aqueous and CO_2 loaded aqueous amine mixtures. The thesis will attempt to highlight the differences of developed correlations with research literature.

The research chapter also shows that the Eyring's viscosity model is often used to develop correlations for the excess free energy of activation for viscous flow and the Gibbs excess free energy. Thus, the thesis will also aim to discuss the possibilities to use vapor-liquid equilibrium models to represent viscosities of amine + water + CO_2 mixtures.

4   Method

The calculation procedures and evaluations of investigated equations for density and viscosity is elaborated in this chapter. Applied measurement data for aqueous mixtures are also included in this section.

4.1 Evaluation of correlations

The curves fitted from measured properties were evaluated by the average absolute relative deviation percentage (AARD%) in Eq (4.1), and the absolute maximum deviation by Eq (4.2). The formulas contain D which represents the number of datapoints and A that includes the measured and calculated properties of a pure or liquid mixture. A low value for AARD indicates low scatter between all measured and calculated datapoints.

$$AARD\% = \frac{100\%}{D} \sum_{i=1}^{D} \left| \frac{A_i^m - A_i^c}{A_i^m} \right| \tag{4.1}$$

$$AMD = MAX|A_i^m - A_i^c| \tag{4.2}$$

The coefficient of determination (R^2), also known as an indicator for the goodness of fit by correlated curves and parameters was obtained by Eq (4.3). The calculation evaluates the sum of squares error (SSE) and the total sum of squares (SST) which includes the average of measurements ($\overline{A^m}$). A value for the coefficient of determination close to 1 indicates a good curve fit in MATLAB.

$$R^2 = 1 - \frac{SSE}{SST} = 1 - \frac{\sum_{i=1}^{D} (A_i^m - A_i^c)^2}{\sum_{i=1}^{D} (A_i^m - \overline{A^m})^2} \tag{4.3}$$

4.2 Measurement data

Calculations involving aqueous mixtures contain density data of pure water at 293.15K – 343.15K from Kestin et al. [36], while the corresponding viscosity of water at datapoints 293.15K – 363.15K were gathered from the work of Korson et al. [37]. The remaining density points at 353.15K and 363.15K were selected from Kell [38], and was found to be reasonable after comparing tested correlations for aqueous MEA to existing models from literature. References to measurement data of amines are included in relevant equations in Chapter 5 and appendices B, C and D to keep a simple overview of the information.

4.3 Calculations

The calculations were performed by using scripts in Python 3.6 and by applying the curve fit application in MATLAB R2020b. For pure amines, the correlation for density and viscosity was performed by the setup of the Python script included in Appendix G.1. The code runs through temperature and density data at a constant mole fraction ($x_1 = 1$).

The script for pure amines was attempted to be modified for aqueous mixtures, but the Curve_fit function in Python was not applicable to 3-dimensional data. Thus, the calculations for aqueous and CO_2 loaded aqueous amines were continued in MATLAB where property data was entered in the Curve Fitting Toolbox as an x, y, z diagram. This included mole fraction ($x_1 = x$), Temperature ($T = y$) and density or viscosity (ρ or $\eta = z$). Within the calculations, the mole fraction of water was treated as a function of the amine ($x_2 = 1 - x_1$). Post-processing of all obtained results was computed in Microsoft Excel to generate graphs and tables. An overview of all studied correlations can be viewed in Table 4.1.

Table 4.1 Overview of all tested correlations.

Property	Components	Correlations	Eq.
Density	MEA, AMP, MDEA, DMEA, DEEA	$$\rho = A + BT + CT^2$$	(3.1)
		$$\rho = \left(k_1 + \frac{k_2 x_2}{T}\right) \exp\left(\frac{k_3}{T^2} + \frac{k_4 x_1}{T} + k_5 \left(\frac{x_1}{T}\right)^2\right)$$ AMP, MDEA, DMEA and DEEA calculation is shown in Appendix B	(3.4)
Viscosity	MEA, AMP, MDEA, DMEA, DEEA	$$ln(\eta) = A + \frac{B}{T}$$	(5.1)
		$$ln(\eta) = A + \frac{B}{T + C}$$	(5.2)
		$$ln(\eta) = A + \frac{B}{T} + \frac{C}{T^2}$$ AMP, MDEA, DMEA and DEEA calculation is shown in Appendix C	(5.3)
Density	Aqueous MEA, Aqueous MDEA	$$\rho_{mixture} = \left(k_1 + \frac{k_2 x_2}{T}\right) \exp\left(\frac{k_3}{T^2} + \frac{k_4 x_1}{T} + k_5 \left(\frac{x_1}{T}\right)^2\right)$$	(3.4)
Density	Aqueous MEA	ρ correlation by V^E is shown in Appendix E. $$\rho = \frac{\left(\sum_1^2 x_i \cdot M_i\right)}{V^E + \left(\sum_1^2 x_i \cdot \frac{M_i}{\rho_i}\right)}$$	(3.5)
		$$V^E = (k_1 + k_2 T + k_3 x_1 + k_4 x_1^2) \cdot x_1 x_2$$	(3.6)

Density	Aqueous MDEA	$$\ln(\rho_d) = \ln(\rho_{mixture}) - \sum_{i=0}^{i=2} x_i \ln(\rho_i)$$	(5.13)
		$$\ln(\rho_d) = x_1 x_2 \sum_{i=0}^{i=n} C_i (1 - 2x_2)^i$$	(5.14)
		$$C_i = a_i + b_i(T)$$	(3.18)
Viscosity	Aqueous MEA, Aqueous MDEA	Testing correlations for (ΔF^{E*}) to represent viscosity of mixtures. $$\ln(\eta V) = \sum_{i=1}^{i=2} x_i \ln(\eta_i V_i) + \frac{\Delta F^{E*}}{RT}$$	(5.4)
		1$^{\text{st}}$ correlation for ΔF^{E*}, estimation of all parameters. $$\frac{\Delta F^{E*}}{RT} = x_1 x_2 \sum_{i=1}^{i=2} C_i (1 - 2x_2)^i$$ $$C_i = a_i + b_i(T)$$	(3.17) (3.18)
		2$^{\text{nd}}$ correlation for ΔF^{E*}, binary temperature parameters given by Aspen Plus V10. $$\frac{\Delta G^{E*}}{RT} = x_1 x_2 \left(\frac{G_{21}\,\tau_{21}}{x_1 + x_2 G_{21}} + \frac{G_{12}\tau_{12}}{x_1 G_{12} + x_2} \right)$$ $$\frac{-\Delta G^{E*}}{\Delta F^{E*}} = a + b \cdot x_1 \cdot T + c \cdot T^2$$	(3.40) (3.43)
		3$^{\text{rd}}$ correlation for ΔF^{E*}, estimation of all parameters. $$\Delta \tilde{G}^{E*} = \Delta F^{E*} \cdot a$$ $$\frac{\Delta \tilde{G}^{E*}}{RT} = \tilde{x}_1 \tilde{x}_2 \left(\frac{G_{21}\,\tau_{21}}{\tilde{x}_1 + \tilde{x}_2 G_{21}} + \frac{G_{12}\tau_{12}}{\tilde{x}_1 G_{12} + \tilde{x}_2} \right) * a$$ $$\tilde{x}_1 = \frac{r_1 x_1}{r_1 x_1 + r_2 x_2}$$	(5.8) (5.7) (5.9)

Viscosity	Aqueous MEA	η correlation is shown in Appendix F. $$\eta = \left[\frac{\sum\left(x_i V_i \eta_i^{\frac{1}{8}}\right)}{\sum(x_i V_i)}\right]^8$$	(3.55)
Density	CO_2 loaded aqueous MEA	$$\rho = (a_1 + a_2(T) + a_3(T^2) + a_4 x_3)\left(k_1 + \frac{k_2 x_2}{T}\right)\exp\left(\frac{k_3}{T} + \frac{k_4 x_1}{T} + k_5\left(\frac{x_1}{T}\right)^2\right)$$	(3.10)
Viscosity	CO_2 loaded aqueous MEA	$$\ln(V\eta)_{CO_2\ loaded} - \ln(V\eta)_{unloaded} = x_3(d_1 + d_2 T + d_3 x_3)$$	(3.19)

5   Calculations and results

This section includes all computations in developing correlations for the density and viscosity of pure, aqueous and CO_2 loaded aqueous amines. The results are displayed through graphs and by calculated deviations from adopted measurement data.

5.1 Density of pure amines

The measured properties of pure MEA was retrieved from research by Karunarathne et al. [17], and applied in creating density correlations by the Polynomial Eq (3.1) and the Aronu, Hartono and Svendsen Eq (3.4). The resulting curves in Figure 5.1 shows that both correlations are quite good at estimating the density in the temperature range 293.15 to 363.15K. Comparing the AARD% and the AMD for both methods, show that the polynomial Eq (3.1) only gives a slightly better fit for the density of pure MEA. The correlations can be viewed in Table 5.1.

With reference to Chapter 3.1 the Polynomial Eq (3.1) :

$$\rho = A + BT + CT^2$$

And Aronu, Hartono and Svendsen correlation Eq (3.4):

$$\rho = \left(k_1 + \frac{k_2 x_2}{T}\right) \exp\left(\frac{k_3}{T^2} + \frac{k_4 x_1}{T} + k_5 \left(\frac{x_1}{T}\right)^2\right)$$
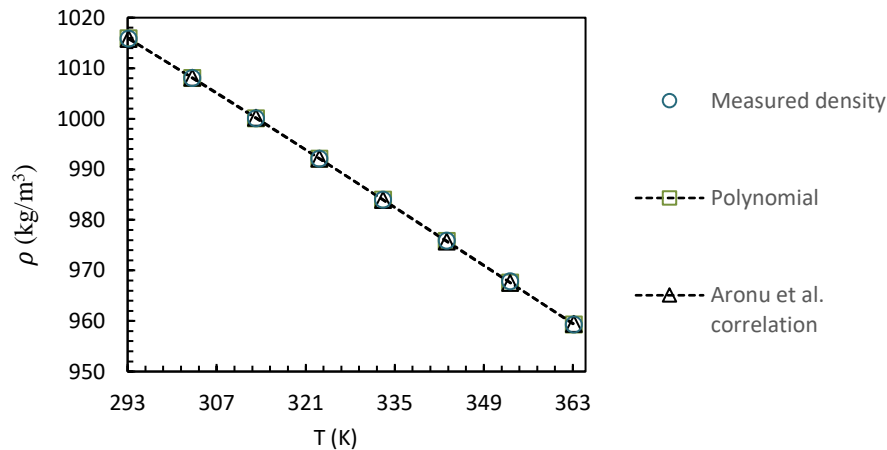

Figure 5.1 Measured vs curve fitted density of pure MEA.

Table 5.1 Parameters of density correlations for pure MEA.

Polynomial		Aronu et al. correlation	
A	1212.4639	k_1	537.04
B	-0.56	k_2	0
C	-0.00038	k_3	17618.02
		k_4	310.76
		k_5	-53944.20
		x_1	1
		x_2	0
AARD %	0.006	AARD %	0.014
AMD (kg/m^3)	0.283	AMD (kg/m^3)	0.355

The procedure was duplicated for other pure amines such as AMP, MDEA, DMEA and DEEA. All calculations can be viewed in Appendix B.

5.2 Viscosity of pure amines

Different versions of the Andrade Eq (3.2) was applied in creating correlations for the viscosity of pure MEA. The original formula contains "$\ln(A)$" which can be interpreted as a constant "A", this matches the Andrade Eq (5.1) found in the research of Karunarathne [39].

$$ln(\eta) = A + \frac{B}{T} \tag{5.1}$$

The work of Karunarathne also includes a modified version of the Andrade equation, which is known as the Vogel Eq (5.2).

$$ln(\eta) = A + \frac{B}{T + C} \tag{5.2}$$

In addition, a second modification, Eq (5.3), can be found in the same research.

$$ln(\eta) = A + \frac{B}{T} + \frac{C}{T^2} \tag{5.3}$$

Applied measurement data were gathered from the same source as the density calculations of pure MEA [17]. Curves and parameters of the viscosity fitting can be viewed in Figure 5.2 and Table 5.2. Results show a significant improvement from the original Eq (3.2) to the Vogel Eq (5.2). The fit continues to improve by a smaller AARD% from the first modification to the second Eq (5.3).
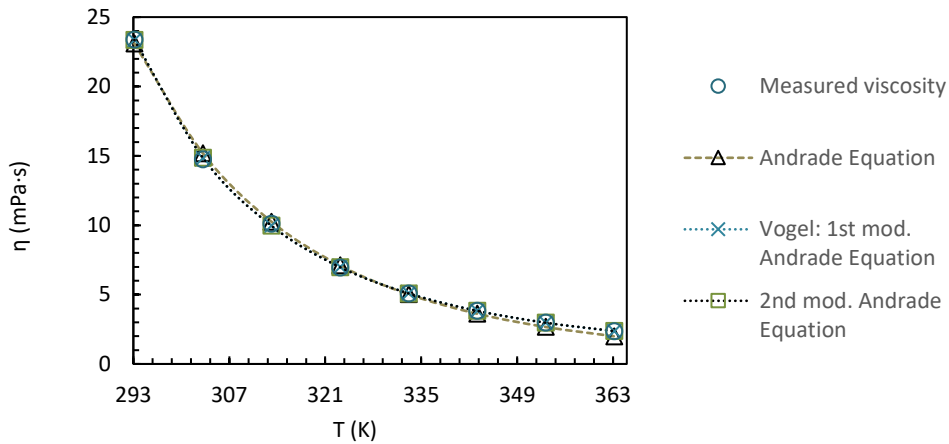
Figure 5.2 Measured vs curve fitted viscosity of pure MEA.

Table 5.2 Parameters for viscosity correlations of pure MEA.

Andrade Equation		Vogel: 1st mod. Andrade Equation		2nd mod. Andrade Equation	
A	-9.57	A	-3.94	A	0.55
B	3724.79	B	1038.02	B	-2602.03
		C	-146.79	C	986263.66
AARD%	5.044	AARD%	0.525	AARD%	0.465
AMD (kg/m^3)	0.434	AMD (kg/m^3)	0.151	AMD (kg/m^3)	0.150

The calculation was also performed for AMP, MDEA and DEEA. The calculations can be found in Appendix C.

5.3 Viscosity of aqueous MEA

The measurements and correlations in the research of Karunarathne et al. was applied in calculations for aqueous MEA. This included following their example of curve fitting excess free energy of activation for viscous flow to be used in viscosity estimation [17]. Applied measurement data of density and viscosity can be found in Appendix D. This data was used to create correlations in the temperature range of 293.15K to 363.15K.

5.3.1 Correlation for density

Measured densities from Karunaratne's research were used to find an expression for the density of aqueous MEA [17]. This was performed by utilizing the Aronu, Hartono and Svendsen correlation from Eq (3.4). The parameters were compared to the findings of Karunarathne in Table 5.3. The curve fit was later used in conjunction with the excess free energy of activation to compute viscosity of aqueous MEA.

Reference to Eq (3.4):

$$\rho = \left(k_1 + \frac{k_2 x_2}{T}\right) \exp\left(\frac{k_3}{T^2} + \frac{k_4 x_1}{T} + k_5 \left(\frac{x_1}{T}\right)^2\right)$$

Table 5.3 Aronu et al. correlation parameters for density of aqueous MEA.

Parameters		
k1	683.7	683.5
k2	134300	134400
k3	-10860	-10890
k4	145	145.2
k5	569.9	567.9
AARD%	0.12	0.12
AMD (kg/m^3)	3.48	3.45
	This work	Karunarathne et al. [17]

The fitted result shown in Figure 5.3 calculated for the MEA mole fraction in the range of 0.1122 to 0.7264 corresponds to a mass ratio of MEA to water within 0.3 to 0.9.
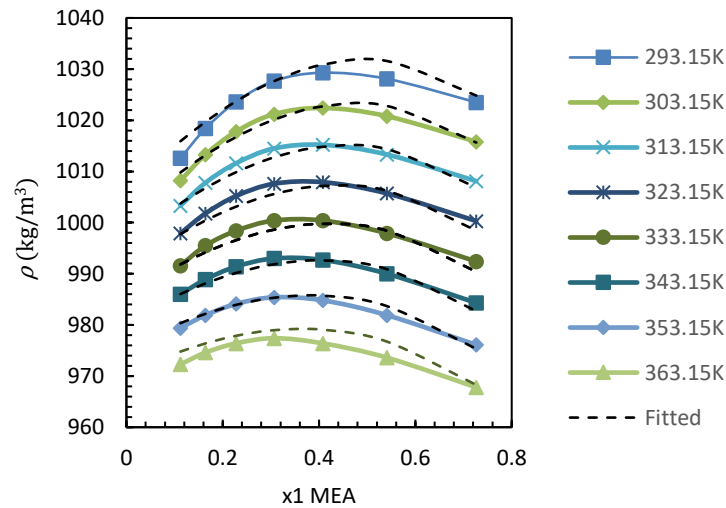

Figure 5.3 Density for aqueous MEA fitted by Aronu et al. correlation.

5.3.2 Eyring's viscosity model

The formula of Eyring's viscosity model in Eq (5.4) was retrieved from research by Karunarathne et al. The model was used in finding the excess free energy of activation for viscous flow [17]. The correlation differs from Eyring's original Eq (3.16) as the excess free energy term is positive.

In this relation, measured viscosity was entered directly into Eq (5.4) while the molecular weight and volume of the mixture was first computed by Eq (5.5) and Eq (5.6). The resulting value for the excess free energy were then used to find parameters in the Redlich-Kister, Eyring-NRTL and segment-based Eyring-NRTL relation in order to calculate the viscosity.

$$\ln(\eta V) = \sum_{i=1}^{i=2} x_i \ln(\eta_i V_i) + \frac{\Delta F^{E*}}{RT} \tag{5.4}$$

$$M_{mixture} = \sum_{i=1}^{i=2} x_i \cdot M_i \tag{5.5}$$

$$V = \frac{M_{mixture}}{\rho_{mixture}}, \quad V_i = \frac{M_i}{\rho_i} \tag{5.6}$$

$i = 1$ for Monoethanolamine (MEA), 2 for water

5.3.3 Redlich-Kister correlation

The proposed Redlich-Kister correlation shown in Eq (3.17) and Eq (3.18) was employed by Karunarathne et al. to create a function for the excess free energy of activation for viscous flow. The computation gave almost identical coefficients as previously found by Karunarathne [17].

A comparison of the parameters and goodness of fit is shown in Table 5.4. The result of this correlation can be viewed in Figure 5.4.

Reference to Chapter 3.4 for liquid viscosity correlations where Eq (3.17) and Eq (3.18) is mentioned:

$$\frac{\Delta F^{E*}}{RT} = x_1 x_2 \sum_{i=1}^{i=2} C_i (1 - 2x_2)^i$$

$$C_i = a_i + b_i(T)$$

Table 5.4 Redlich-Kister correlation for excess free energy of activation for aqueous MEA.

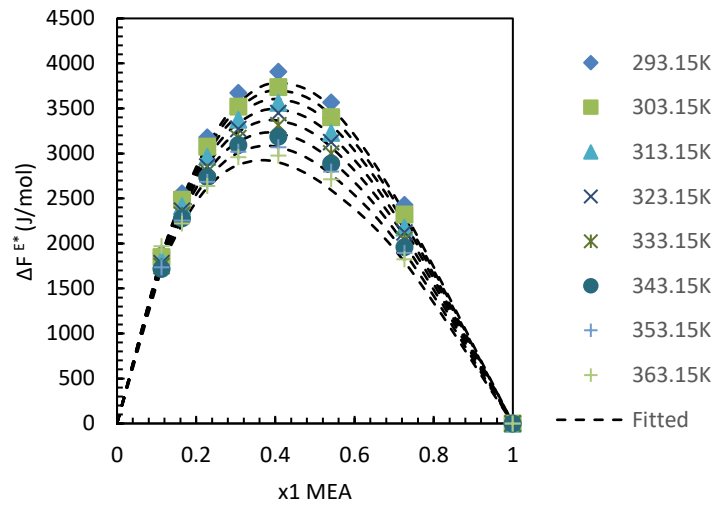|	Coefficients	
a0	16.04	16.02
a1	-4.766	-4.853
a2	-6.592	-6.433
b0	-0.03425	-0.03473
b1	0.008053	0.008315
b2	0.02113	0.02065
R^2	0.9967	0.998
	This work	Karunarathne et al.

Figure 5.4 Fitted Redlich-Kister model for the excess free energy of activation for aqueous MEA.

The Redlich-Kister model and the values from the density correlation were then applied to estimate the viscosity. As shown by the comparison in Figure 5.5, the viscosity can be calculated through creating a function for the excess free energy of activation and the density.

The results were obtained by using Eq (5.4) to solve for the viscosity (η). This included inserting ΔF^{E*} = Redlich-Kister correlation and $\rho_{mixture}$ = Aronu et al. correlation. The viscosity correlation resulted in an AARD% of 2.39 and an AMD of 0.84.
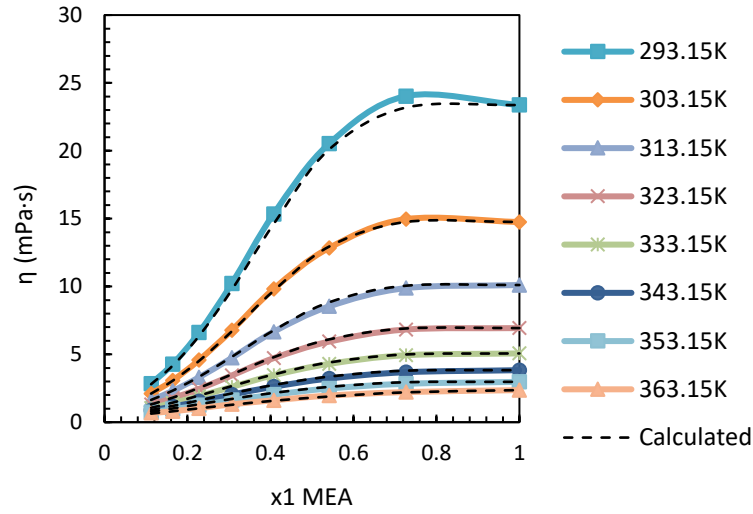
Figure 5.5 Comparison of measured and calculated viscosity by Redlich-Kister correlation for aqueous MEA.

5.3.4 Eyring-NRTL model

The NRTL model from Eq (3.40) was used to test the Eyring-NRTL correlation by Novak mentioned in Chapter 3.4.1.3. The model was used with binary temperature dependent parameters from a mixture simulation in Aspen Plus version 10 with components MEA (x_1) and H_2O (x_2, distilled water). The simulated values a through f were entered in Eq (3.44) and (3.45) to calculate Gibbs excess free energy (ΔG^{E*}). The computation was then attempted to be fitted in Eyring's viscosity model as the excess free energy of activation (ΔF^{E*}).

The applied Eq (3.40), (3.41) is listed below:

$$\frac{\Delta G^{E*}}{RT} = x_1 x_2 \left(\frac{G_{21}\,\tau_{21}}{x_1 + x_2 G_{21}} + \frac{G_{12}\tau_{12}}{x_1 G_{12} + x_2} \right)$$

$$G_{ij} = \exp\left(-\alpha_{ij} \cdot \tau_{ij}\right)$$

Which includes Eq(3.44) and (3.45):

$$\tau_{ij} = a_{ij} + \frac{b_{ij}}{T} + e_{ij} \ln T + f_{ij} T$$

$$\alpha_{ij} = c_{ij} + d_{ij}(T - 273.15K)$$

Choosing the run mode "analysis" in Aspen Plus gave binary parameters of aqueous MEA in Table 5.5, valid for a temperature range of 298.15K to 384.85K. The resulting curve for Gibbs excess free energy is shown in Figure 5.6.

Table 5.5 NRTL parameters from Aspen Plus for aqueous MEA.

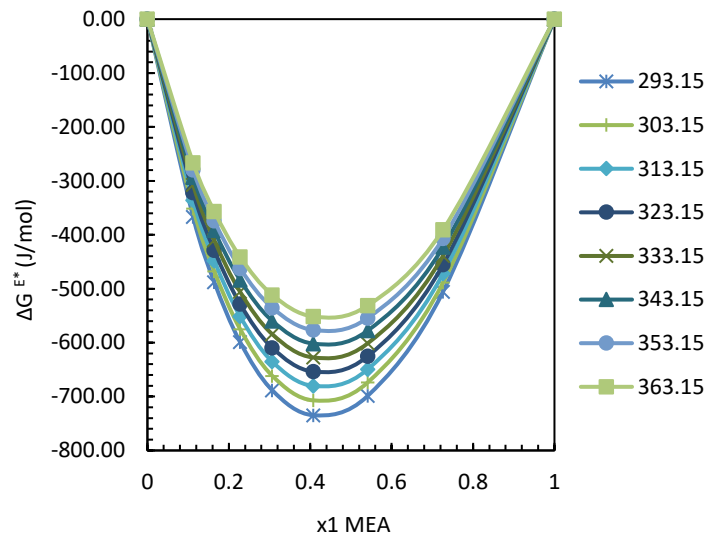| APV100 parameters	
A_{12}	-0.0352
A_{21}	1.1605
B_{12}	-438.061
B_{21}	-110.329
$C_{12} = C_{21}$	0.3
D_{ij}, E_{ij}, F_{ij}	0

Figure 5.6 Gibbs excess free energy for aqueous MEA by Aspen Plus NRTL parameters.

While comparing the calculated Gibbs excess free energy (ΔG^{E*}) to the excess free energy of activation (ΔF^{E*}) as computed by Chapter 5.3.2, it became evident that the results varied too much to be used interchangeably. The correlation in Eq (3.43) by Karunarathne and Øi was therefore applied [29]. The formula was originally used for binary parameters from literature, and during this thesis Karunarathne proposed to try the same correlation for the estimated parameters from Aspen Plus. The resulting fit to the excess free energy of activation in Table 5.6 and Figure 5.7 was then used to calculate the viscosity through Eyring's viscosity model and density correlation from Chapter 5.3.1. A reference to Eq (3.43) is given below:

$$\frac{-\Delta G^{E*}}{\Delta F^{E*}} = a + b \cdot x_1 \cdot T + c \cdot T^2$$

Table 5.6 Parameters developed to Karunarathne et al. correlation for Gibbs excess free energy of aqueous MEA.

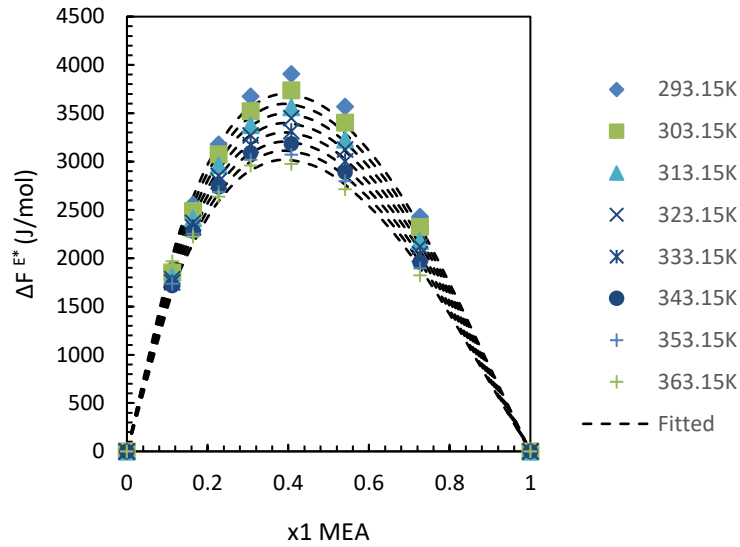| Coefficients	
a	0.2157
b	0.0001957
c	-4.674E-07
R^2	0.8441

Figure 5.7 Excess free energy of activation for aqueous MEA fitted from Gibbs excess free energy by Aspen Plus NRTL parameters.

The proposed correlation by Karunarathne et al. combined with the Eyring-NRTL model gave an AARD% of 1.87 and an AMD of 1.45 for the viscosity of aqueous MEA. The results can be viewed in Figure 5.8.
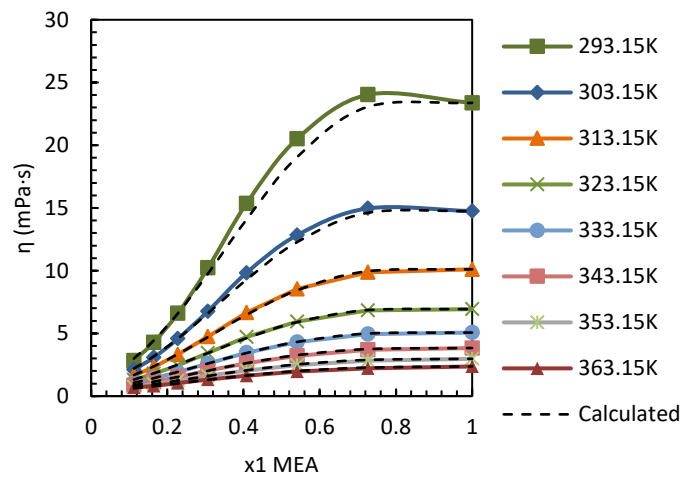

Figure 5.8 Comparison of measured and calculated viscosity of aqueous MEA by Aspen Plus NRTL parameters.

5.3.5 Segment-based Eyring-NRTL model

As previously mentioned in Chapter 3.4.1.3, Novak et al. also created a segment-based Eyring -NRTL model based on the theory that larger molecules flow in segments. The model differs from the Eyring-NRTL model by an additional correlation for the mole fraction of the first component [20]. The segment-based model was in this thesis attempted to be curve fitted to prepared data of excess free energy of activation for aqueous MEA. The calculation proved to be difficult without an additional correlation and thus the constant "a" were suggested by the main supervisor of this thesis, Sumudu Karunarathne, to be added in Eq (5.7). This can be viewed as a relation between the segment-based Gibbs excess free energy ($\Delta\tilde{G}^{E*}$) and the excess free energy of activation for viscous flow (ΔF^{E*}).

$$\frac{\Delta\tilde{G}^{E*}}{RT} = \tilde{x}_1\tilde{x}_2\left(\frac{G_{21}\,\tau_{21}}{\tilde{x}_1 + \tilde{x}_2 G_{21}} + \frac{G_{12}\tau_{12}}{\tilde{x}_1 G_{12} + \tilde{x}_2}\right) * a \tag{5.7}$$

$$\Delta\tilde{G}^{E*} = \Delta F^{E*} \cdot a \tag{5.8}$$

The Gibbs excess free energy in Eq (5.7) is as mentioned above based on segments of moles instead of component moles. This is reflected in Eq (5.9) where r represents the average number of segments in the components. For a case where the solvent is viewed as a componentet, r_2 can be set equal to 1.

$$\tilde{x}_1 = \frac{r_1 x_1}{r_1 x_1 + r_2 x_2} \tag{5.9}$$

$$\tilde{x}_2 = 1 - \tilde{x}_1 \tag{5.10}$$

G_{12} and G_{21} in Eq (3.41) includes the interaction energies (τ) between the two different components and the nonrandomness factor (α) which is identical for both cases:

$$G_{12} = \exp\left(-\alpha_{12}\tau_{12}\right)$$

$$G_{21} = \exp\left(-\alpha_{12}\tau_{21}\right)$$

$\tau_{12}\ and\ \tau_{21}$ were set to correlations (5.11) shown in the article on the use of the NRTL equation by Schmidt, Maham and Mather [30].

$$\tau_{12} = a_{12} + \frac{b_{12}}{T} \qquad \tau_{21} = a_{21} + \frac{b_{21}}{T} \tag{5.11}$$

The relation of the Eyring-NRTL model and the segment-based is shown in Eq (5.12).

$$\frac{\Delta G^{E*}}{RT} = \frac{N}{N_s}\frac{\Delta\tilde{G}^{E*}}{RT} \tag{5.12}$$

All parameters from Eq (5.7) - (5.11) and (3.41) was estimated by curve fitting the segment-based Eyring-NRTL model to the excess free energy of activation for aqueous MEA as calculated through Chapter 5.3.2. The result is shown in Table 5.7 and Figure 5.9.

Table 5.7 Segment -based Eyring-NRTL correlation for excess free energy of activation for viscous flow – aqueous MEA.

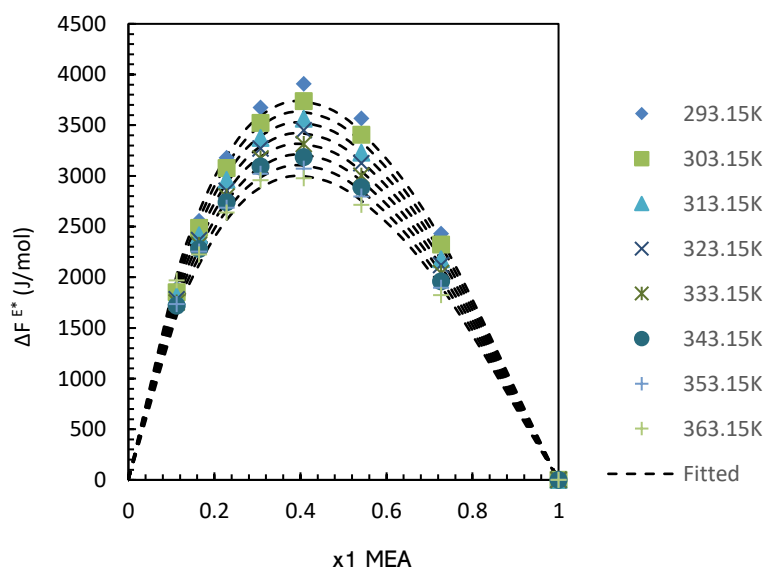| Parameters	
a	-8.173
a12	0.2936
a21	0.3271
α12	4.56E-11
b12	-403.6
b21	1.712
r	1.52
R^2	0.995

Figure 5.9 Fitted excess free energy of activation from the Segment-based Eyring NRTL model for aqueous MEA.

The values from the fitted Segment-based model and the result from the Aronu et al. density correlation was then used in the calculation of the viscosity. Figure 5.10 shows the comparison of the calculated and measured result. The relation gave an AARD% of 1.88 and an AMD of 1.04.
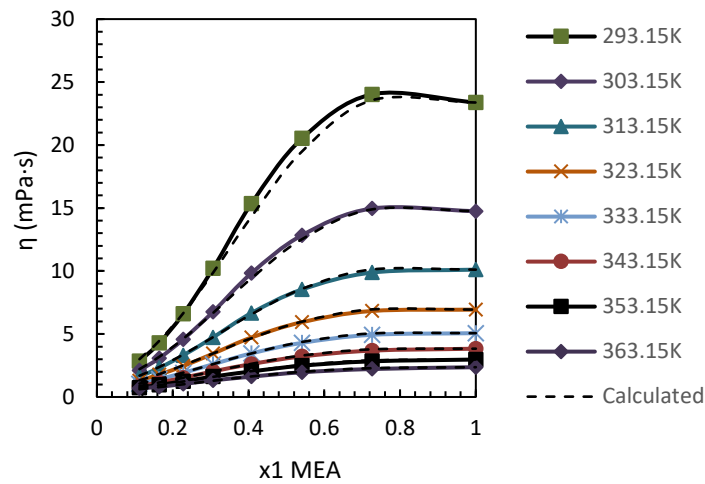
Figure 5.10 Comparison of measured and calculated viscosity by the segment-based Eyring-NRTL model for aqueous MEA.

5.3.5.1 Evaluation of the Segment-based model

During the fitting of the segment-based model for aqueous MEA, some problems with the relation was noticed. The incredibly small value of α12 in the parameter overview in Table 5.7 essentially renders G_{21} and G_{12} redundant, as the Eq (3.41) reduces to the value of 1.

$$G_{12} = \exp(0 \cdot \tau_{12}) = 1$$
$$G_{21} = \exp(0 \cdot \tau_{21}) = 1$$

The results imply that Eq (5.7) could be reduced to a function without G_{21} and G_{12}, which would exclude the nonrandomness parameter (α) from the correlation.

$$\frac{\Delta \tilde{G}^{E*}}{RT} = \tilde{x}_1 \tilde{x}_2 \left(\frac{\tau_{21}}{\tilde{x}_1 + \tilde{x}_2} + \frac{\tau_{12}}{\tilde{x}_1 + \tilde{x}_2} \right) * a$$

The formula appeared to work better for Aqueous MEA if the entire formula was multiplied by -1, and if parameters α12, b12 and r were set to contain positive numbers. Resulting in the parameters by Table 5.8 for Eq (5.7) - (5.11) and (3.41).

Table 5.8 Segment-based Eyring-NRTL model correlation improved for aqueous MEA.

Coefficients	
a	-1
a12	-14.89
a21	16.71
α12	0.041
b12	4827
b21	-6891
r	1.675
R^2	0.9979

The alternative correlation gave a high coefficient of determination (R^2) with the value of 0.9979, meaning that the fit for excess free energy of activation for viscous flow for aqueous MEA became slightly better than with the Redlich-Kister correlation.

5.4 Viscosity of aqueous MDEA

The correlations for aqueous MDEA was developed by using measurement data in the temperature range of 293.15K to 343.15K from the research of Karunarathne, Eimer and Øi [40]. The calculations were performed by applying the same methods as used for aqueous MEA in Chapter 5.3. This included utilizing fitted curves of density and excess free energy of activation to estimate viscosity. The data was also in this case prepared by initially calculating the excess free energy of activation through Eyring's viscosity model as mentioned in Chapter 5.3.2.

5.4.1 Correlation for density

The Aronu et al. correlation from Eq (3.4) was also tested for aqueous MDEA but did not give a very good fit for the density. The equations were therefore changed to fit the density deviation to a Redlich-Kister polynomial, similar to the correlation applied to excess free energy of activation shown in Chapter 3.4. The approach in Eq (5.13) was proposed by Karunarathne, Eimer and Øi [40].

$$\ln(\rho_d) = \ln(\rho) - \sum_{i=0}^{i=2} x_i \ln(\rho_i) \tag{5.13}$$

For practical reasons when calculating, Eq (5.13) can be rewritten as shown below.

$$\ln(\rho_d) = \ln\left(\rho \cdot \rho_1^{-x_1} \cdot \rho_2^{-x_2}\right)$$

The density deviation can then be fitted to a Redlich-Kister polynomial (5.14) in the same manner as shown in Chapter 5.3.2 by applying Eq (3.18) for C_i.

$$\ln(\rho_d) = x_1 x_2 \sum_{i=0}^{i=n} C_i (1 - 2x_2)^i \qquad (5.14)$$

With reference to the Eq (3.18) used in Chapter 5.3.2:
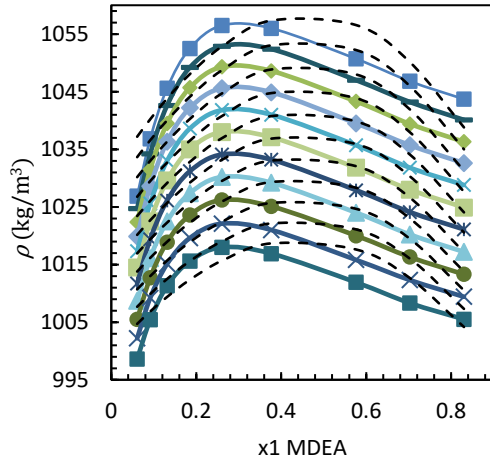
$$C_i = a_i + b_i(T)$$

Figure 5.11 Density of aqueous MDEA fitted by Aronu et al. correlation.
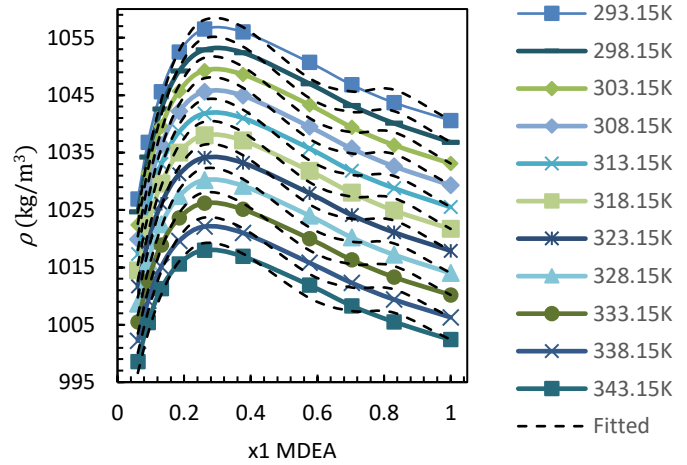
Figure 5.12 Density of aqueous MDEA fitted by a deviation to Redlich-Kister polynomial.

The fit improved drastically from Figure 5.11 to Figure 5.12 by applying the Redlich-Kister polynomial. The obtained parameters and deviation calculations can be viewed in Table 5.9.

Table 5.9 Parameters for density correlations of aqueous MDEA.

Aronu et al. correlation, ρ		Redlich-Kister polynomial, $\ln(\rho_d)$	
k_1	749.6	a_0	0.3223
k_2	102300	a_1	-0.4282
k_3	-5492	a_2	0.4197
k_4	126	b_0	-6.795E-04
k_5	-5327	b_1	8.728E-04
		b_2	-8.291E-04
AARD %	0.35	AARD %	0.15
AMD (kg/m^3)	10.29	AMD (kg/m^3)	2.76

5.4.2 Redlich-Kister correlation

The procedure of Chapter 5.3.2 were followed in fitting the calculated excess free energy of activation for viscous flow of aqueous MDEA to the Redlich-Kister correlation by Eq (3.17) and (3.18). The result can be viewed in Table 5.10 and Figure 5.13.

Table 5.10 Redlich-Kister correlation for excess free energy of activation for viscous flow of aqueous MDEA.

Coefficients	
a0	30.45
a1	-20.4
a2	5.081
b0	-0.06844
b1	0.04439
b2	-0.003935
R^2	0.9977

The coefficients found in Table 5.10 by applying the Redlich-Kister correlation gives a high coefficient of determination, meaning that this is a good fit.
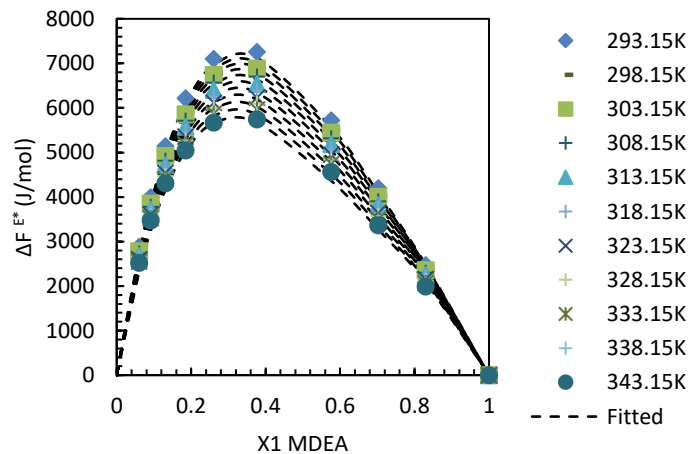

Figure 5.13 Fitted Redlich-Kister model for the excess free energy of activation for aqueous MDEA.

Similar to the calculations for aqueous MEA in Chapter 5.3.2, the procedure of calculating the viscosity from the fitted results of excess free energy of activation for viscous flow and density was applied. The resulting calculation in Figure 5.14 gave an AARD% of 3.04 and an AMD of 7.19.
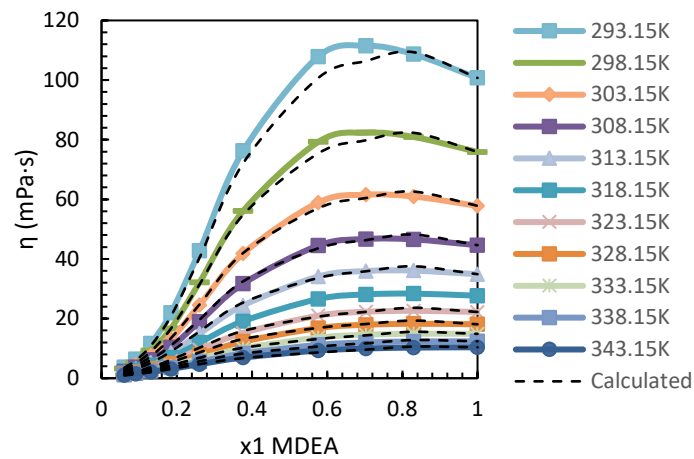
Figure 5.14 Comparison of measured and calculated viscosity by Redlich-Kister correlation for aqueous MDEA.

5.4.3 Eyring-NRTL model

Aspen Plus Version 10.0 (APV100) was applied in calculating the Gibbs excess free energy of aqueous MDEA by following the procedure of Chapter 5.3.4. This included using Eq (3.40), (3.41), (3.44) and (3.45). A simulation was performed to estimate values a through f for the mix of components MDEA and H_2O ("distilled water"). Running a regular analysis gave no results to the binary parameters and changing the mode to run by estimation supplied parameters which were only valid for 298.15K. The source in estimation mode were therefore changed to NISTV100 NIST-IG (version 10.0 database). This gave a broader temperature range of 278.95 to 478.7K.

The parameters from Aspen Plus given in Table 5.11 was used in Eq (3.44) and (3.45). The resulting Gibbs excess free energy can be seen in Figure 5.15.

Table 5.11 NRTL parameters from Aspen Plus for aqueous MDEA.

NISTV100 NIST-IG parameters	
A_{12}	4.75322
A_{21}	-1.79134
B_{12}	159.444
B_{21}	-716.787
$C_{12} = C_{21}$	0.1
D_{ij}, E_{ij}, F_{ij}	0

Calculated values were then used to create the correlation between Gibbs excess free energy and excess free energy of activation for viscous flow by Eq (3.43) in Table 5.12.

Table 5.12 Parameters developed to Karunarathne et al. correlation for Gibbs excess free energy of aqueous MDEA.

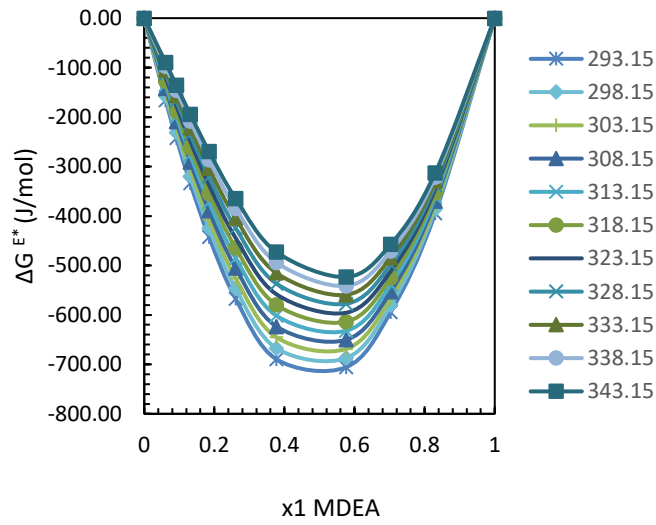| Coefficients	
a	0.1089
b	0.0004605
c	-7.107E-07
R^2	0.9989

Figure 5.15 Gibbs excess free energy for aqueous MDEA by Aspen Plus NRTL parameters.
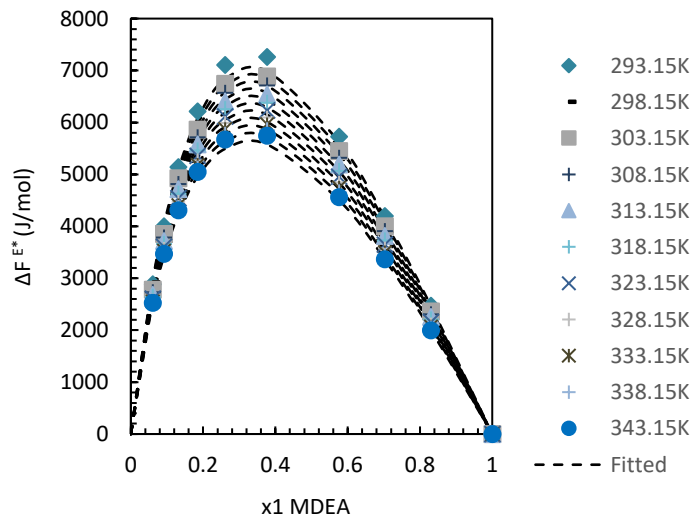
Figure 5.16 Excess free energy of activation fitted from Gibbs excess free energy of aqueous MDEA by Aspen Plus NRTL parameters.

Results from the correlation by Eq (3.43) were then used in Eyring's viscosity model with the density correlation from Chapter 5.4.1 to calculate the viscosity of aqueous MDEA in Figure 5.17. The calculation gave an AARD% of 2.23 and an AMD of 8.05.

Figure 5.17 Comparison of measured and calculated viscosity for aqueous MDEA by Aspen Plus NRTL parameters.

5.4.4 Segment-based Eyring-NRTL model

The viscosity of aqueous MDEA was also calculated by fitting excess free energy of activation for viscous flow to the segment-based Eyring-NRTL model and by using results from the fitted density by the Redlich-Kister correlation in Chapter 5.4.1.
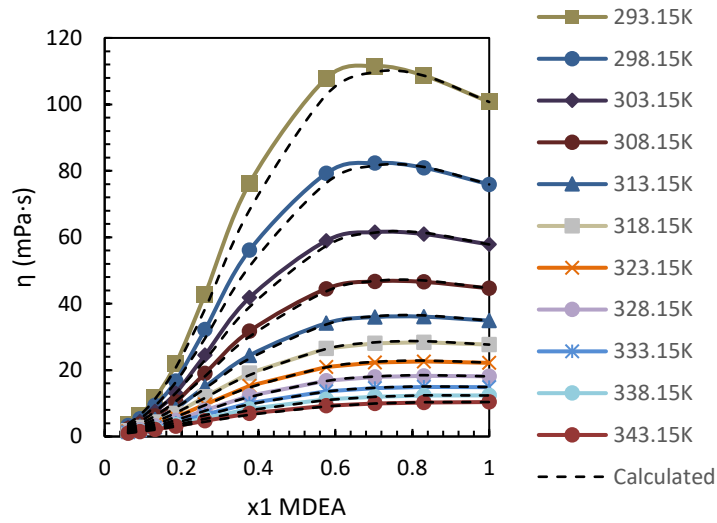
Following the same calculation as Chapter 5.3.5, gave acceptable parameters in even though the computation in MATLAB did not converge through a high number of maximum iterations. This caused parameters to change each time the calculation was performed.
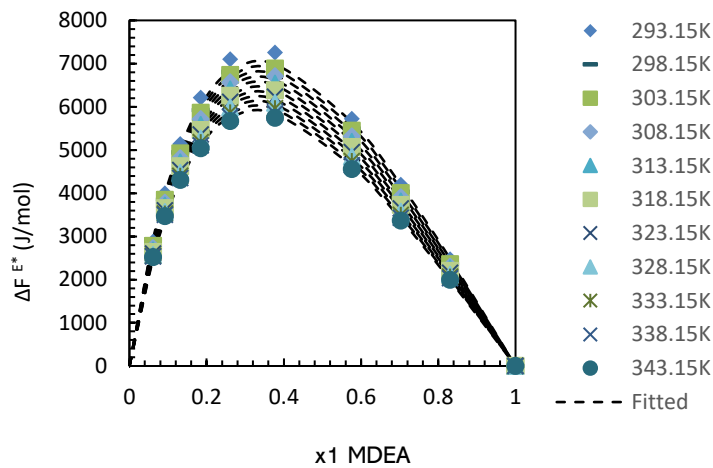
Figure 5.18 Fitted excess free energy of activation from the Segment-based Eyring-NRTL model for aqueous MDEA.

The segment-based Eyring-NRTL model shown in Figure 5.18 included parameters from Table 5.13.

Table 5.13 Parameters for segment-based Eyring-NRTL model for excess free energy of activation for viscous flow of aqueous MDEA.

Parameters	
a	1
a12	-2.504
a21	-3.817
α12	-0.101
b12	1596
b21	2937
r	2.349
R^2	0.9988

The result was used to portray the viscosity in Figure 5.19, where the calculated values gave an AARD% of 1.88 and an AMD of 8.07.

Figure 5.19 Comparison of calculated and measured viscosity of aqueous MDEA through the Segment-based Eyring-NRTL model.

5.5 Density of CO₂ loaded aqueous MEA

The density correlation of Aqueous MEA by Aronu, Hartono and Svendsen mentioned in Chapter 3.3 can be expanded to contain a function for CO_2 loading. This was done in the work by Karunar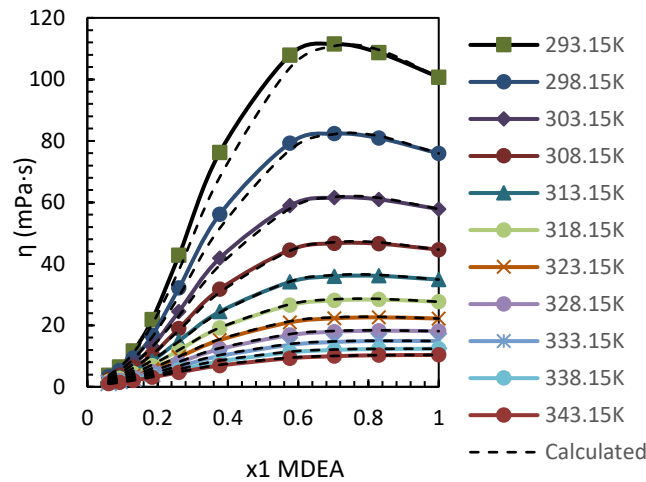athne, Eimer and Øi which resulted in Eq (3.10) [17]. This correlation is based on the results from the Aronu et al. relation. Where all k_i values are equal to the given values in Chapter 5.3.1. The function relates CO_2 loading (ψ = mol CO_2/mol MEA) by mole fraction (x_3) to MEA and water (x_1 and x_2).

Eq (3.10) is recited below:

$$\rho = (a_1 + a_2(T) + a_3(T^2) + a_4 x_3) \left(k_1 + \frac{k_2 x_2}{T} \right) \exp\left(\frac{k_3}{T} + \frac{k_4 x_1}{T} + k_5 \left(\frac{x_1}{T} \right)^2 \right)$$

The function was fitted to CO_2 loaded density data at 293.15 to 323.15K and applied to the mole fraction of MEA at values 0.1122 and 0.1643 in the temperatures range 293.15 to 353.15K. Higher temperatures were omitted from the fitting as the measurement data was not available at $x_3 = 0.0826$ from 333.15 to 353.15K. Results are presented in Table 4.4 and Figures 4.14 and 4.15.

Table 5.14 Comparing results of this work vs research by Karunarathne et al. [17].

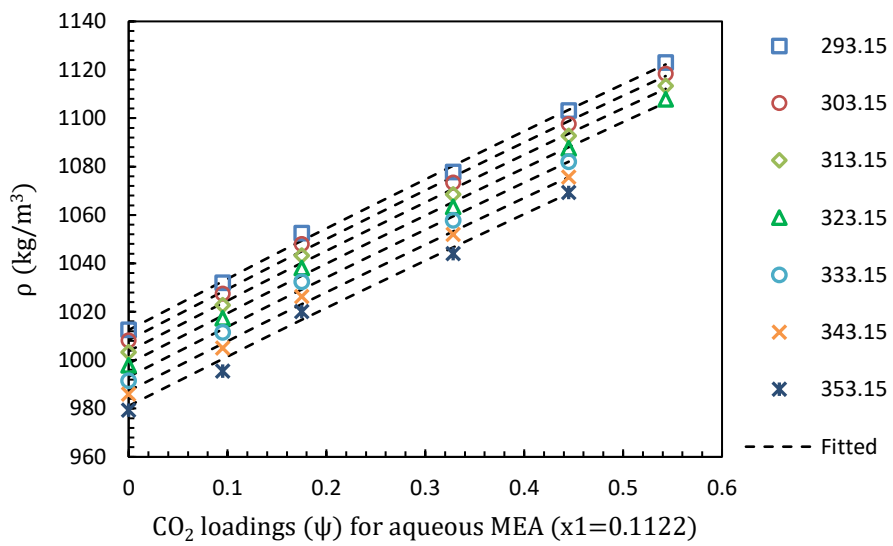|	Parameters			
	$x_1 = 0.1122, w_1 = 0.3$		$x_1 = 0.1643, w_1 = 0.4$	
a_1	0.7209	0.6802	0.7494	0.7731
a_2	0.001664	0.001951	0.001469	0.001354
a_3	-2.47E-06	-2.97E-06	-2.13E-06	-2.015E-06
a_4	1.882	2.346	1.657	2.164
AARD%	0.15	0.15	0.09	0.08
AMD (kg/m^3)	4.94	4.2	3.33	2
	This work	Karunarathne et al.	This work	Karunarathne et al.

Figure 5.20 Correlation for density by CO_2 loading at a mass ratio (w_1) of 0.3 between MEA and water.

Figure 5.21 Correlation for density by CO_2 loading at a mass ratio (w_1) of 0.4 between MEA and water.

5.6 Viscosity of CO₂ loaded aqueous MEA

The relation by Karunarathne et al. from Eq (3.19) was used to correlate the viscosity of CO_2 loaded aqueous MEA. This was done through utilizing the density and viscosity of both aqueous MEA and CO_2 loaded aqueous MEA. The correlation was performed with measurement data from the same source as applied in Chapter 5.5 in the range 293.15K to 353.15K [17]. The correlation contains density measurements of CO_2 loaded aqueous MEA through Eq (5.15), thus it also became necessary in this case to omit values for $x_3 = 0.0826$ at 333.15 to 353.15K.

Reference to Eq (3.19):

$$\ln(V\eta)_{CO_2\ loaded} - \ln(V\eta)_{unloaded} = x_3(d_1 + d_2T + d_3x_3)$$

$$V_{CO_2\ loaded} = \frac{\sum_1^3(x_i \cdot M_i)}{\rho_{CO_2\ loaded}} \tag{5.15}$$

The result of this correlation is shown in Table 5.15, where the correlation for a mass ratio between MEA and water of 0.3 is shown in Figure 5.22 while Figure 5.23 shows the mass ratio of 0.4.

Table 5.15 Comparing results of curve fitted viscosity for CO_2 loaded aqueous MEA in this work vs research by Karunarathne et al. [17].

	Parameters			
	$x_1 = 0.1122, w_1 = 0.3$		$x_1 = 0.1643, w_1 = 0.4$	
d_1	7.135	4.536	8.925	2.554
d_2	0.002273	0.006765	-0.005609	0.01205
d_3	5.741	12.08	18.52	19.46
AARD%	0.53	0.58	1.66	1.13
AMD (kg/m^3)	0.03	0.03	0.12	0.22
	This work	Karunarathne et al.	This work	Karunarathne et al.

Figure 5.22 Correlation for viscosity by CO_2 loading at a mass ratio (w_1) of 0.3 between MEA and water.
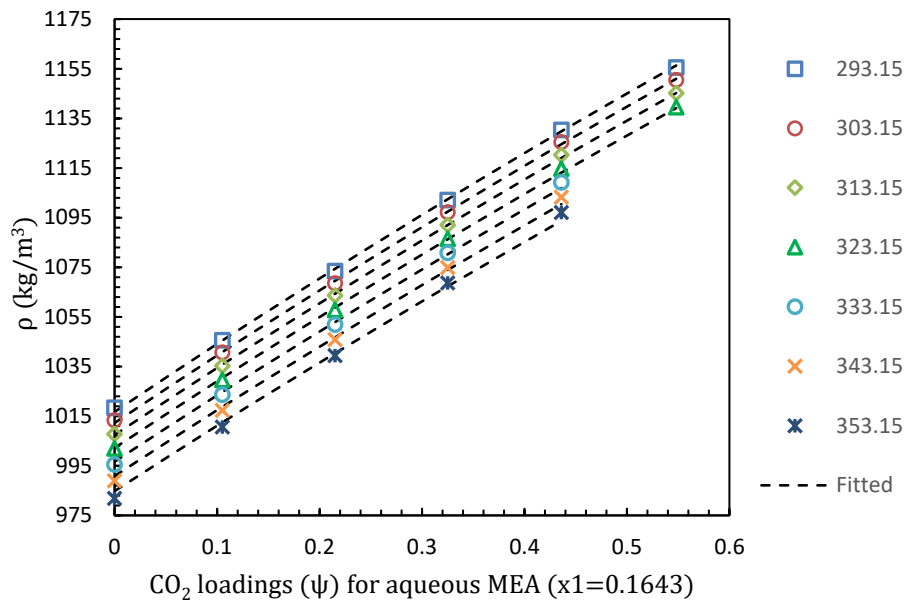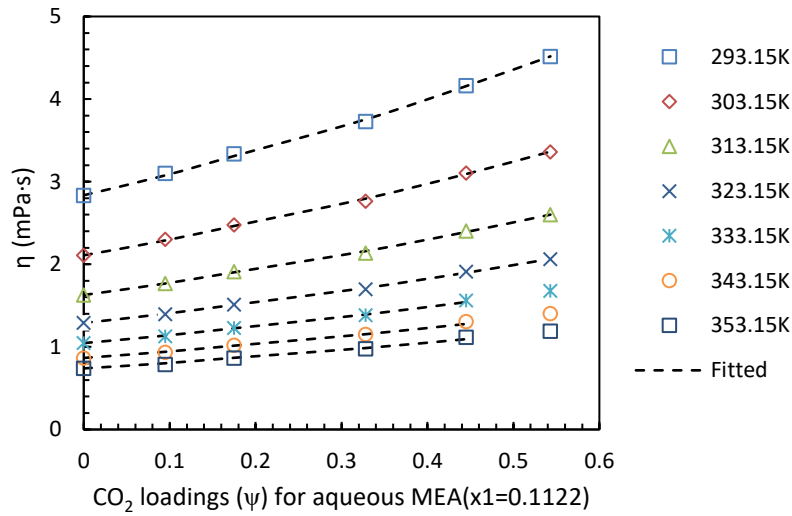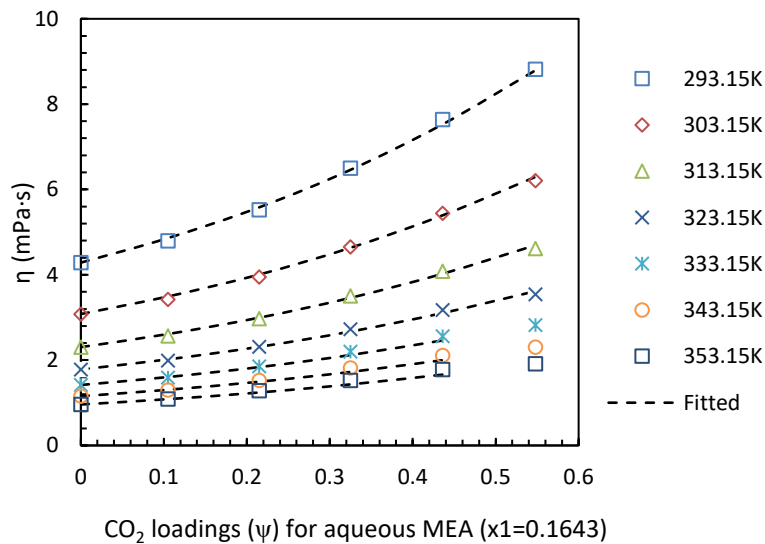

Figure 5.23 Correlation for viscosity by CO_2 loading at a mass ratio (w_1) of 0.4 between MEA and water.

6 Discussion

The discussion entails correlations found in literature, summarizing findings in this thesis and evaluates the applicability of VLE models to represent viscosities.

6.1 Correlations

6.1.1 Pure liquids

Results from density correlations of pure amines in Table 6.1 show that the polynomial Eq (3.1) gave the best fit for MEA and DMEA, while the calculations for MDEA and DEEA show that the two applied methods gave very similar results. Inversely, the density of AMP appeared to be better fitted to the Aronu et al. correlation. Overall, the results show that the polynomial equation can be deemed sufficient for the 5 considered amine types.

Table 6.1 Comparison of applied density correlations in this work for pure amines

Component	Polynomial Eq (3.1)		Aronu et al. correlation Eq (3.4)	
	AARD%	AMD	AARD%	AMD
MEA	0.006	0.283	0.014	0.355
AMP	0.010	0.244	0.006	0.185
MDEA	0.007	0.155	0.007	0.160
DMEA	0.009	0.197	0.011	0.211
DEEA	0.012	0.316	0.012	0.329

Applying 3 different versions of the Andrade Eq (3.2) for viscosity showed enhanced correlations with each modification. The overview in Table 6.2 reveal that the 2nd modification gave the best results for MEA, AMP, MDEA and DEEA. For DMEA, the first and second modification gave almost equal results. Considering the AARD%, the 2nd modification was found the most accurate to portray the viscosities of the pure amines.

Table 6.2 Comparison of applied viscosity correlations in this work for pure amines

Component	Andrade Eq (5.1)		Vogel Eq (5.2)		Andrade 2nd mod Eq (5.3)	
	AARD%	AMD	AARD%	AMD	AARD%	AMD
MEA	5.044	0.434	0.525	0.151	0.465	0.150
AMP	5.080	0.727	0.395	0.073	0.184	0.045
MDEA	5.752	1.084	0.572	0.252	0.362	0.213
DMEA	0.578	0.014	0.124	0.007	0.125	0.007
DEEA	2.153	0.057	0.406	0.015	0.338	0.014

6.1.2 Binary mixtures

The Aronu et al. density correlation by Eq (3.4) works quite well for aqueous MEA but was not applicable for mole fraction values above 0.7264 [17]. The model was in addition tested for aqueous MDEA which unfortunately provided poor results. If more precise values covering the range from highly aqueous MEA to pure MEA are required, the Hartono et al. correlation from Eq (3.5) and (3.6) could be applied. The comparison in Table 6.3, shows that the correlation by Hartono et al. can achieve an AARD of 0.03% and an AMD of 1.06 for aqueous MEA. For the calculation of density for aqueous MDEA, the Redlich-Kister correlation gave an AARD of 0.15%. In comparison, the original work by Karunarathne et al. found an AARD of 0.1% [40].

Table 6.3 Density of aqueous MEA - comparison of AARD% for different methods.

Reference	Method	AARD%	AMD
This work	Aronu et al. correlation Eq (3.4)	0.12	3.45
Karunarathne et a. [17]	Aronu et al. correlation Eq (3.4)	0.12	3.45
This work	Hartono et al. correlation by Eq (3.5) and (3.6) in Appendix E	0.03	1.06
Hartono et al. [16]	Eq (3.5) and (3.6)	0.04	Not found

The calculation for the viscosity of aqueous MEA was computed by values from research of Karunarathne et al [17]. The major difference in AARD% in this work and by Karunarathne et al. was the choice of inserting the density correlation in Eyring's viscosity model when calculating viscosity from the excess free energy of activation for viscous flow (ΔF^{E*}). The compared methods of calculating the viscosity of aqueous MEA can be viewed in Table 6.4. The results show that including the density correlation in the calculation of viscosity affects the AARD% by almost 1% extra.

Table 6.4 Viscosity of aqueous MEA - comparison of AARD% for different methods.

Reference	Method	No. Parameters	AARD%
This work	Density correlation via Eq (3.4) and Redlich-Kister correlation for ΔF^{E*} by Eq (3.17).	11	2.39
Karunarathne et al. [17]	Redlich-Kister correlation for ΔF^{E*} by Eq (3.17).	6	1.4
Hartono et al. [16]	Simplified Redlich-Kister correlation for viscosity (η) - Eq (3.12).	4	4.2

As stated, correlations for the viscosity of aqueous MEA were performed with a consistent correlation. This was done to compare the methods in Table 6.5. The same procedure was

followed for aqueous MDEA in Table 6.6. An initial guess during the calculations was that the Redlich-Kister model for the excess free energy of activation (ΔF^{E*}) would give the best fit compared to other methods. Considering that the relation is a higher degree polynomial and showed a very low average maximum deviation (AMD). The AARD% on the other hand gave the highest result for this model, possibly due to having fewer parameters to estimate.

Reviewing research literature by Novak et al. in Chapter 3.4.1.3 for the Eyring-NRTL model showed that the Gibbs excess free energy was fronted with a negative prefix. how would this change the outcome of calculations in Chapter 5.3.4 and 5.4.3? The calculations for aqueous MEA and aqueous MDEA were performed by treating the excess free energy of activation as a positive value. Following Novak's example could result in a simpler correlation between the excess free energy of activation and Gibbs excess free energy.

The Segment-based Eyring-NRTL model had a high number of available parameters, which in turn gave a very good fit to the viscosity of aqueous MEA and aqueous MDEA. Although the method seemed to fit quite well, the problem with this method is that it initially gave invalid parameters in MATLAB for the excess free energy of activation for aqueous MEA. This led to the idea of correlating Gibbs excess free energy by a constant "a". For aqueous MDEA, the same constant was given the value of 1. Thus, an unconstricted estimation of all parameters was not attainable. Additionally, the nonrandomness (α) is considered by literature to contain an empirical value between 0.1-0.9 [30]. From the calculation concerning aqueous MEA, the nonrandomness parameter was as low as 4.56E-11, while the same value showed up negative for aqueous MDEA.

Table 6.5 Comparing methods of correlating ΔF^{E*} and ρ to viscosity of aqueous MEA.

	Redlich-Kister model	Eyring-NRTL by Aspen parameters	Segment-based Eyring NRTL model
No. Parameters for density (ρ)	5		
No. Parameters for ΔF^{E*}	6	8 (5 from Aspen Plus)	7
AARD%	2.39	1.87	1.88
AMD (kg/m^3)	0.84	1.45	1.04

Table 6.6 Comparing methods of correlating ΔF^{E*} and ρ to viscosity of aqueous MDEA.

	Redlich-Kister model	Eyring-NRTL by Aspen parameters	Segment based Eyring NRTL model
No. Parameters for density (ρ)	6		
No. Parameters for ΔF^{E*}	6	8 (5 from Aspen Plus)	7
AARD%	3.04	2.23	1.88
AMD (kg/m^3)	7.19	8.05	8.07

6.1.3 Ternary mixtures

The calculations containing CO_2 loaded aqueous MEA was fitted to specific mol fractions of MEA, i.e. a mass ratio between MEA and water corresponding to 0.3 and 0.4. The result of the density correlations in Table 6.7 showed that the relation by Karunarathne et al. gave a very good fit. The Hartono et al. relation only gave a slightly better fit by an AARD of 0.13%. The difference in the calculations might be narrowed down to Hartono et al. considering the volume expansion when the 3 components are mixed.

The correlation for the viscosity of CO_2 loaded aqueous MEA was also performed by a relation proposed by Karunarathne et al. In this case, parameters were found to be similar but not identical. It is not clear what caused the values in this thesis to differ. Even if the parameters had a large mismatch, the AARD% was quite similar. Table 6.8 also shows that the Karunarathne et al. correlation works better than the Hartono et al. model for viscosity.

Although the empirical relations applied to CO_2 loaded aqueous MEA was considered good, the methods do not consider ions formed during the mixing of these components. The only reviewed model which addressed the reactions was the VLE based Electrolyte-NRTL correlation when connected to Eyring's viscosity model.

Table 6.7 Density correlations for CO_2 loaded aqueous MEA

Reference	Method	No. Parameters	AARD%	
This work	Aronu et al. correlation expanded in Eq (3.10)	9	0.15	0.09
Karunarathne et al. [17]	Aronu et al. correlation expanded in Eq (3.10)	9	0.15	0.08
Hartono et al. [16]	Eq (3.7), (3.8) and (3.9)	3	0.13	Not found
Mass ratio (*w*) between MEA and water			0.3	0.4

Table 6.8 Viscosity correlations for CO_2 loaded aqueous MEA

Reference	Method	No. Parameters	AARD%	
This work	Eq (3.16) and (5.15)	3	0.53	1.66
Karunarathne et al. [17]	Eq (3.16) and (5.15)	3	0.58	1.13
Hartono et al. [16]	Eq (3.20) and (3.21)	3	2.00	Not found
Mass ratio (*w*) between MEA and water			0.3	0.4

6.1.4 Relation independent of temperature

An attempt to fit the viscosity data of aqueous MEA was performed by Bhatt's relation through Eq (3.55) in Appendix F. Unfortunately, the result appeared to show a slightly linear curve whereas the viscosity of aqueous MEA shows a more curved behavior for mole fractions between 0.1 and 1. Thus the model was not investigated further.

6.2 Vapor-liquid equilibrium models

Researched VLE models in this thesis showed that regressing measurement data is necessary to create adequate relations to estimate viscosity. For the promising model UNIFAC-VISCO which could be used with only pure component data, Pooling et al. does not recommend using the method on systems containing water [26]. Considering this aspect, a possible solution to apply the method UNIFAC-VISCO to CO_2 loaded aqueous amine systems could be to create a new correlation for the interaction parameters. This idea was based on Chevalier et al. mentioning for one mixture that the temperature variations in calculating the interaction parameters could be excluded to give better results [27].

The electrolyte-NRTL model can be viewed as the most appropriate model for acid gas systems as it covers all the reactions between CO_2, MEA and water. In this thesis, the model was attempted to be fitted against experimental values from the research of Karunarathne by following the method of Matins et al. in Chapter 3.4.1.4, but it became evident that the model requires more in-depth knowledge on how to apply the interaction parameters from Aspen Plus to the different terms of the equations.

For the Eyring-NRTL model, it was shown in Chapter 5.3.4 and 5.4.3 that it is possible to use VLE data in calculating the viscosity of the aqueous amines by using an additional correlation from the work of Karunarathne et al. [29]. Unfortunately, it was not well understood how the interaction parameters for the CO_2 loaded aqueous amines would be estimated in Aspen Plus for the NRTL Eq (3.40). Therefore, the simulation was not expanded to include CO_2 loaded mixtures. Continuing to the segment-based version of the Eyring-NRTL model, estimations of viscosity for aqueous amines was performed with a correction factor. For this case, it was also not well understood how the NRTL Eq (3.40) is applied to 3 components.

The last reviewed VLE model, Eyring-UNIQUAC researched by Wu and Martins et al., seems to be possible to apply to aqueous amines without major issues. This would include following the same procedure as performed for the Eyring-NRTL model, switching the estimation method to UNIQUAC for the interaction parameters. Unfortunately, the timeframe of this thesis did not make it possible to continue exploring the model.

6.3 Computational tools

The curve fitting script from the SciPy package in Python 3.6 appears to be created for 2 dimensional arrays [41]. This created problems during the task of fitting 3 variables (mole fraction, temperature and property data) to a given function. The script created in Appendix G.1 is therefore only applicable to pure property values. The work-around to find optimized parameters for the Aronu et al. correlation for density in Eq (3.4), was therefore to use the numerical "Nelder-Mead" method [42]. This includes iteratively searching for the minimum or maximum value for unknown parameters in a function. Appendix G.2 shows the script created by Finn Aakre Haugen which can be applied in cases with 3-dimensional data. The method was deemed rather complex for this master thesis as it required a guess of initial values for parameters, and additional work to change the code for each case. The calculation software for mixtures was therefore continued with MATLAB R2020b. The undeniable advantage of using the MATLAB curve fit application instead of Python is that it provides a user-friendly interface that makes it possible to perform a series of calculations at a faster pace.

7   Conclusion

Physicochemical properties are important in designing CO_2 capture modules as it can affect the mass transfer of CO_2 and the packing height of absorption/desorption columns. In this thesis, it was also found that viscosity seems to have a greater impact than density in the CO_2 capture process.

The polynomial Eq (3.1) and the 2nd Andrade modification Eq (5.3) can be considered adequate to respectively represent density and viscosity of pure amines. The developed script in Appendix G.1 can be applied to find parameters in these equations. For aqueous amines, promising correlations for one type might not be applicable to other aqueous amines. This was observed by Eq (3.4) where the Aronu et al. correlation applied to density of aqueous MEA gave deficient results for aqueous MDEA.

In correlating viscosity for aqueous amines, the applied methods of Redlich-Kister, Eyring-NRTL and segment-based Eyring-NRTL gave an AARD% of 2.39, 1.87 and 1.88 for aqueous MEA. The same methods gave an AARD% of 3.04, 2.23 and 1.88 for aqueous MDEA. The results imply that the performed calculations connected to the NRTL model worked better for both mixtures. The applied Eyring-NRTL model was connected to a relation by Karunarathne et al. which made it feasible to apply estimated VLE data from Aspen Plus. In the segment-based Eyring-NRTL correlation, the estimation of all parameters was made possible by a correction factor.

For CO_2 loaded aqueous MEA, the two empirical relations proposed by Karunarathne et al. was tested and found to provide adequate values for density and viscosity. For a mass ratio of 0.3 between MEA and water, the correlations gave an AARD% of 0.15 and 0.53 respectively. The relations estimated physicochemical properties in terms of CO_2 loading.

Most of the researched vapor-liquid equilibrium models include the assumption that density measurements are readily available in the prediction of viscosity, except for the UNIFAC-VISCO model. Instead, the relation by Chevalier et al. used the molecular weight of all components. Unfortunately, the correlation was not advised by Pooling et al. for water mixtures. Further research showed that the Electrolyte-NRTL model evaluates all ion formations in the mixture of amine, water and CO_2. The latter VLE relation could be effective in predicting viscosities of CO_2 loaded aqueous amines with the use of Aspen Plus.

In this thesis, MATLAB was considered the most effective tool for calculations including 3-dimensional data (x_1, temperature and viscosity or density). This was concluded as Python requires the development of a more complex scripts to perform the same computations.

7.1 Future work

The timespan of this work limited the possibility of further researching the setup of all interaction energies for the Electrolyte-NRTL model in Aspen Plus. Out of curiosity it would be interesting to find more information on how all equation terms correlate for the molecule and ion interactions. This could be used to test the applicability of the model for viscosity of CO_2 loaded aqueous amines in conjunction with simulated VLE values.

As a continuation of the research work, it would also be interesting to test if a new correlation for the interaction parameters in the UNIFAC-VISCO model could make the model applicable to the viscosity of CO_2 loaded aqueous amines. The correlation is known as a zero-parameter model but seeing as it is not advised to be applied to water mixtures the additional correlation could expand the area of application.

Another suggestion would be to simulate interaction parameters in Aspen Plus to compute the viscosity of binary and ternary liquids in the Eyring-UNIQUAC model. The trials could be done by comparing the equations of Wu and Martins et al. to determine which model works better in conjunction with Aspen Plus software. Results could indicate if the change by Martins et al. to the ideal term in Eyring's viscosity model is reasonable.

As a last proposition for further work, the segment-based Eyring-NRTL model could be tested in MATLAB by restricting the interaction parameters to the recommended value range given in literature. The test could also include how the correlation between the excess free energy of activation and Gibbs excess free energy would change by treating this term as negative in Eyring's viscosity model.

References

[1] IEA, "Global Energy Review 2021 - CO_2 emissions," 19 04 21. [Online]. Available: https://www.iea.org/reports/global-energy-review-2021/CO₂-emissions. [Accessed 07 09 21].

[2] Norwegian Petroleum Directorate, "Emissions and the environment," 27 09 19. [Online]. Available: https://www.npd.no/fakta/publikasjoner/rapporter/ressursrapporter/ressursrapport-2019/utslipp-og-miljo/. [Accessed 31 03 21].

[3] Equinor, "Supporting the transition to a low-carbon society with electrification of oil and gas platforms," 28 02 21. [Online]. Available: https://www.equinor.com/en/what-we-do/electrification.html. [Accessed 24 03 21].

[4] National Energy Technology Laboratory, DOE/NETL carbon capture program - Carbon dioxide capture handbook, Albany: U.S. Department of Energy, 2015, p. 12.

[5] A. J. Kidnay and W. R. Parrish, Fundamentals of Natural Gas Processing, 1st ed., Boca Raton: Taylor and Francis Group, 2006, pp. 96-100.

[6] A. Raksajati, M. Ho and D. Wiley, "Solvent Development for Post-Combustion CO_2 Capture: Recent Development and Opportunities," *MATEC Web Conf.: The Regional Symposium on Chemical Engineering,* vol. 156, no. 03015, p. 8, 2018.

[7] H. Ling, H. Gao and Z. Liang, "Comprehensive solubility of N2O and mass transfer studies on an effective reactive N, N-dimethylethanolamine (DMEA) solvent for post-combustion CO_2 capture," *Chemical Engineering Journal,* vol. 355, pp. 369-379, 01 01 2019.

[8] P. N. Sutar, P. D. Vaidya and E. Y. Kenig, "Activated DEEA solutions for CO_2 capture - A study of equilibirum and kinetic characteristics," *Chemical Engineering Science,* vol. 100, pp. 234-241, 30 08 2013.

[9] B. P. Mandal, A. K. Biswas and S. S. Bandyopadhyay, "Absorption of carbon dioxide into aqueous blends of 2-amino-2-methyl-1-propanol and diethanolamine," *Chemical Engineering Science,* vol. 58, pp. 4137-4144, 14 April 2003.

[10] W. Conway, S. Bruggink, Y. Beyad, W. Luo, I. Melián-Cabrera, G. Puxty and P. Feron, "CO_2 Absorption Into Aqueous Amine Blended Solutions Containing Monoethanolamine (MEA), N,N-dimethylethanolamine (DMEA), N,N-diethylethanolamine (DEEA) and 2-amino-2-methyl-1-propanol (AMP) for Post Combustion Capture Processes," *Chemical Engineering Science,* vol. 126, pp. 446-454, 2015.

[11] D. Song, F. A. Seibert and G. T. Rochelle, "Effect of liquid viscosity on mass transfer area and liquid film mass transfer coefficient for GT-OPTIMPAK 250Y," *Energy Procedia, GHGT-13,* vol. 114, pp. 2713-2727, 2017.

[12] W. Nookuea, Impacts of thermo-physical properties on chemical absorption for CO_2 capture, Västerås: Mälardalen University Press Licentiate Theses, 2016, pp. 44 (19-27).

[13] H. A. Al-Ghawas, D. P. Hagewiesche, G. Ruiz-Ibanez and O. C. Sandall, "Physicochemical Properties Important for Carbon Dioxide Absorption in Aqueous Methyldiethanolamine," *Journal of Chemical & Engineering Data,* vol. 34, no. 4, pp. 385-391, 1989.

[14] E. N. d. C. Andrade, "The Viscosity of Liquids," *Nature,* vol. 125, pp. 582-584, 12 04 1930.

[15] U. E. Aronu, A. Hartono and H. F. Svendsen, "Density, viscosity, and N2O solubility of aqueous amino acid salt and amine amino acid salt solutions," *The Journal of Chemical Thermodynamics,* vol. 45, no. 1, pp. 90-99, 2012.

[16] A. Hartono, E. O. Mba and H. F. Svendsen, "Physical Properties of Partially CO_2 Loaded Aqueous Monoethanolamine (MEA)," *Journal of Chemical & Engineering Data,* vol. 59, no. 6, pp. 1808-1816, 2014.

[17] S. S. Karunarathne, D. A. Eimer and L. E. Øi, "Density, viscosity and free energy of activation for viscous flow of monoethanol amine(1)+H_2O(2)+CO_2(3) mixtures," Fluids, 2020.

[18] R. E. Powell, W. E. Roseveare and H. Eyring, "Diffusion, Thermal Conductivity, and Viscous Flow of Liquids," *Industrial and Engineering Chemistry,* vol. 33, no. 4, pp. 430-435, 1941.

[19] L. T. Novak, "Modeling the Viscosity of Liquid Mixtures: Polymer-Solvent Systems," *Industrial & Engineering Chemistry Research,* vol. 42, no. 8, pp. 1824-1826, 06 03 2003.

[20] C. Chau-Chyun, N. T. Lawrence and S. Yuhua, "Segment-Based Eyring-NRTL Viscosity Model for Mixtures Containing Polymers," Industrial & Engineering Chemistry Research, Washington DC, 2004.

[21] J. M. Smith, H. C. Van Ness and M. M. Abbott, "Excess property, Appendix H: UNIQUAC and UNIFAC equation," in *Introduction to chemical Engineering Thermodynamics*, 7th ed., New York, McGraw-Hill, 2005, pp. 412-413, 791-792.

[22] R. J. Martins, M. J. E. d. M. Cardoso and O. E. Barcia, "Calculation of Viscosity of Ternary and Quaternary Liquid Mixtures," *Industrial & Engineering Chemistry Research,* vol. 40, no. 4, pp. 1271-1275, 31 January 2001.

[23] R. C. Dubey, Advanced Biotechnology, 1st ed., New Delhi: S.Chand & Company Pvt Ltd, 2014.

[24] D. T. Wu, "Prediction of viscosities of liquid mixtures by a group contribution method," *Fluid Phase Equilibria,* vol. 30, pp. 149-156, 1986.

[25] R. J. Martins, M. J. d. M. Cardoso and O. E. Barcia, "Excess Gibbs Free Energy Model for Calculating the Viscosity of Binary Liquid Mixtures," *Industrial & Engineering Chemistry Research,* vol. 39, no. 3, pp. 849-854, 29 01 2000.

[26] B. E. Poling, J. M. Prausnitz and J. P. O'Connell, The properties of gases and liquids, 5th ed., New York: McGraw-Hill, 2001, p. 8.17.

[27] Y. Gaston-Bonhomme, P. Petrino and J. L. Chevalier, "UNIFAC-VISCO Group Contribution Method for Predicting Kinematic Viscosity: Extension and Temperature Dependence," *Chemical Engineering Science,* vol. 49, no. 11, pp. 1799-1806, 20 October 1993.

[28] A. Fredenslund, R. L. Jones and J. M. Prausnitz, "Group-Contribution Estimation of Activity Coefficients in Nonideal Liquid Mixtures," *AIChE Journal,* vol. 21, no. 6, pp. 1086-1099, November 1975.

[29] S. S. Karunarathne and L. E. Øi, "Applicability of NRTL model for prediction of the viscosity of alkanolamine + water mixtures," *Proceedings of The 60th SIMS Conference on Simulation and Modelling SIMS 2019,* vol. 11, no. 170, pp. 73-77, 2019.

[30] K. A. G. Schmidt, Y. Maham and A. E. Mather, "Use of the NRTL Equation for Simultaneous Correlation of Vapour-Liquid Equilibria and Excess Enthalpy - Applications to aqueous alkanolamine systems," Journal of Themal Analysis and Calorimetry, Bergen, Alberta, 2007.

[31] N. J. Matin, J. E. Remias and K. Liu, "Application of Electrolyte-NRTL Model for Prediction of the Viscosity of Carbon Dioxide Loaded Aqueous Amine Solutions," *Industrial & Engineering Chemistry Research,* vol. 52, pp. 16979-16984, 4 November 2013.

[32] D. M. Austgen, G. T. Rochelle, X. Peng and C.-C. Chen, "Model of Vapor-Liquid Equilibria for Aqueous Acid Gas-Alkanolamine Systems Using the Electrolyte-NRTL Equation," *Industrial & Engineering Chemistry Research,* vol. 28, no. 7, pp. 1060-1073, 1989.

[33] J. Herrmann, "Process modeling of novel amine carbon capture solvents," Norwegian University of Science and Technology: Department of Energy and Process Engineering, Trondheim, 2014.

[34] B. D. Bhatt, "Preamble and Applicability of a New Relation for the Estimation of Viscosity of Liquid Mixtures," vol. 56, no. 1, pp. 410-418, 2021.

[35] J. Newton Friend, "Viscosity and Chemical Constitution," *Nature,* vol. 150, p. 432, 10 October 1942.

[36] J. Kestin, M. Sokolov and W. A. Wakeham, "Viscosity of liquid water in the range - 8°C to 150°C," *Journal of Physical and Chemical Reference Data,* vol. 7, no. 3, pp. 941-948, 1978.

[37] L. Korson, W. Drost-Hansen and F. J. Millero, "Viscosity of Water at Various Temperatures," *The Journal of Physical Chemistry,* vol. 73, no. 1, pp. 34-39, 1968.

[38] G. S. Kell, "Density, Thermal Expansivity, and Compressibility of Liquid Water from 0° to 150°C: Correlations and Tables for Atmospheric Pressure and Saturation Reviewed and Expressed on 1968 Temperature Scale," *Journal of Chemical and Engineering Data,* vol. 20, no. 1, pp. 97-105, 1975.

[39] S. S. Karunarathne, "Physicochemical data for amine based CO_2 capture process," University of South-Eastern Norway, Porsgrunn, 2020.

[40] S. S. Karunarathne, D. A. Eimer and L. E. Øi, "Density, Viscosity and Excess Properties of MDEA+H_2O, DMEA+H_2O and DEEA+H_2O mixtures," *Applied Sciences,* vol. 10, no. 9, p. 3196, 2020.

[41] The SciPy community, "SciPy documentation," 20 01 2021. [Online]. Available: https://docs.scipy.org/doc/scipy/reference/generated/scipy.optimize.curve_fit.html. [Accessed 24 01 2021].

[42] F. Gao and L. Han, "Implementing the Nelder-Mead simplex algorithm with adaptive parameters," *Springer,* vol. 51, pp. 259-277, 04 May 2010.

[43] S. S. Karunarathne, L. E. Øi and D. A. Eimer, "Density, viscosity and free energy of activation for viscous flow of CO_2 loaded AMP, MEA and H_2O mixtures," *Journal of Molecular Liquids,* vol. 311, no. 113286, pp. 2-6, 2020.

[44] S. S. Karunarathne, D. A. Eimer, K. J. Jens and L. E. Øi, "Density, Viscosity and Excess Properties of Ternary Aqueous Mixtures of MDEA + MEA, DMEA + MEA and DEEA + MEA," *Fluids,* vol. 5, no. 27, pp. 5-10, 2020.

[45] S. A. Kelayeh, C. Ghotbi and V. Taghikhani, "Correlation of Viscosity of Aqueous Solutions of Alkanolamine Mixtures Based on the Eyring's Theory and Wong-Sandler Mixing Rule," vol. 32, no. 2, 2013.

Appendices

Appendix A: Task description

Appendix B: Density correlations for pure amines

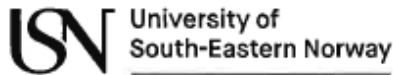Appendix C: Viscosity correlations for pure amines

Appendix D: Measured data of aqueous MEA

Appendix E: Density correlation by Hartono et al. for aqueous MEA

Appendix F: Viscosity correlation by Bhatt for aqueous MEA

Appendix G: Python 3.6 codes for curve fitting of density data

Appendix A: Task description

University of South-Eastern Norway

Faculty of Technology, Natural Sciences and Maritime Sciences, Campus Porsgrunn

FMH606 Master's Thesis

Title: Mathematical models for the physicochemical properties of different solvents of amine based post combustion capture

USN supervisor: Sumudu Karunarathne(main supervisor), Lars Erik Øi (co-supervisor)

Task background:
Physicochemical properties of solvents for amine-based post combustion capture play a vital role in designing of process equipment and process simulations. Properties like density, viscosity and surface tension are appeared in mass transfer and interfacial area correlations developed for both random and structures packing that are used in absorber columns. The mathematical correlations for density and viscosity of both Amine + H_2O + CO_2 mixtures are useful to estimate the properties for the unmeasured conditions. The correlations to represent properties at different species compositions and temperatures makes it possible to consider the effect of density, viscosity and surface tension variations on mass transfer of CO_2 between gas and liquid phases in an absorber column.

Task description:
- Do a literature search for the theoretical, semi empirical and empirical models for density and viscosity of pure and liquid mixtures in process simulation tools.
- Develop semi empirical or empirical correlations for density and viscosity of both aqueous and CO_2 loaded aqueous amine mixtures. The Eyring's viscosity model can be adopted to fit data in literature and develop correlations for the free energy of activation for viscous flow.
- Discuss the possibilities to use VLE (vapour and liquid equilibrium) model represent viscosities of Amine + Water + CO_2 mixtures.
- Evaluate the developed correlations with the correlations available in literature.
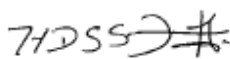
Student category: EET and PT students

The task is suitable for online students (not present at the campus): Yes

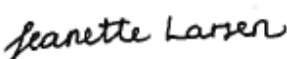**Practical arrangements**: -

Supervision:
As a general rule, the student is entitled to 15-20 hours of supervision. This includes necessary time for the supervisor to prepare for supervision meetings (reading material to be discussed, etc).

Signatures:

Supervisor (date and signature): 27.09.21

Student (write clearly in all capitalized letters): JEANETTE LARSEN

Student (date and signature): 24.09.21

Appendix B: Density correlations for pure amines

Appendix B.1: Density of pure AMP

Measured data applied to the calculation was retrieved from research by Karunarathne et al. [43]. Density correlations was performed with Eq (3.1) and (3.4).
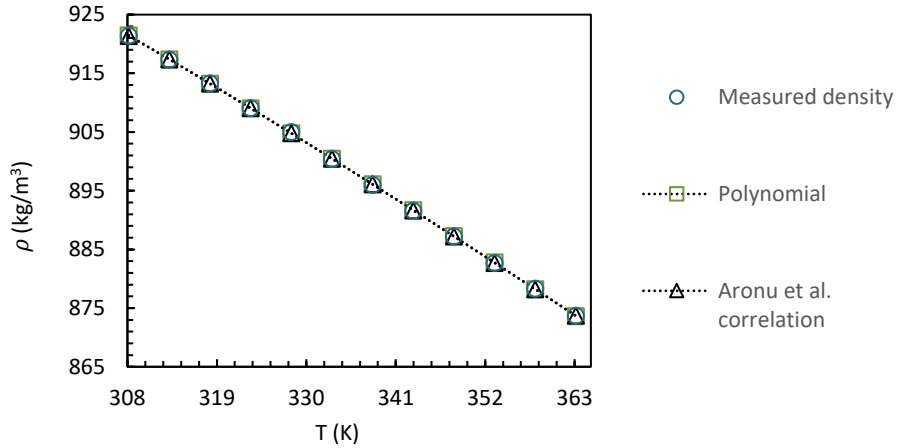
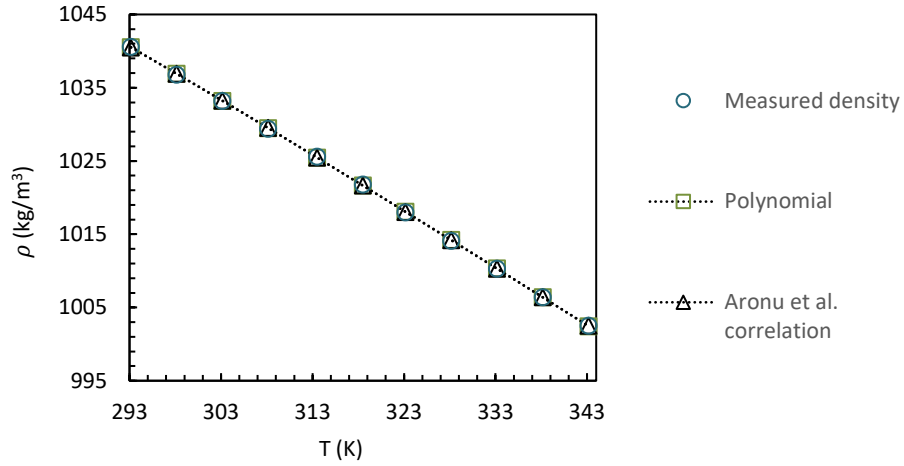| Polynomial		Aronu et al. correlation	
A	1082.2314	k_1	394.71
B	-0.23	k_2	0
C	-0.00096	k_3	-169268.62
		k_4	441.78
		k_5	113628.07
		x_1	1
		x_2	0
AARD %	0.010	AARD %	0.006
AMD (kg/m^3)	0.244	AMD (kg/m^3)	0.185

Appendix B.2: Density of pure MDEA

Measured data applied to the calculation was retrieved from research by Karunarathne et al. [44]. Density correlations was performed with Eq (3.1) and (3.4).

Polynomial			Aronu et al. correlation		
A	1197.09		k_1	579.66	
B	-0.34		k_2	0	
C	-0.00067		k_3	93694.22	
			k_4	284.66	
			k_5	-126867.32	
			x_1	1	
			x_2	0	
AARD %	0.007		AARD %	0.007	
AMD (kg/m^3)	0.155		AMD (kg/m^3)	0.160	

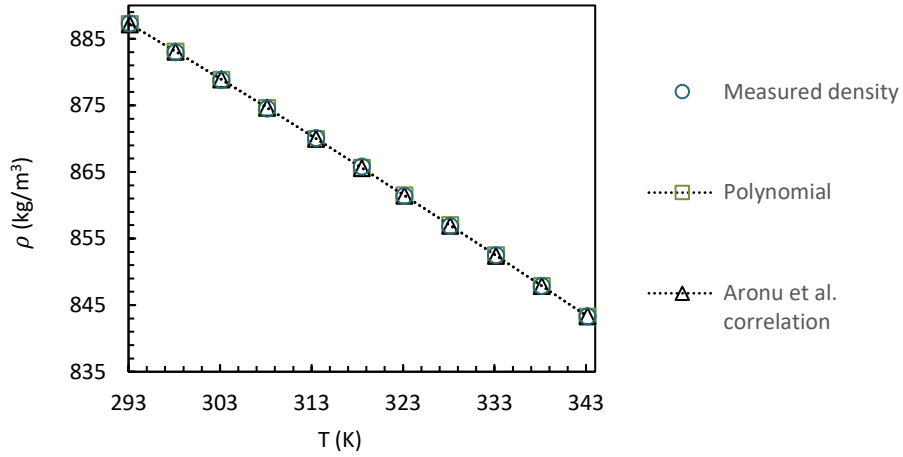## **Appendix B.3: Density of pure DMEA**

Measured data applied to the calculation was retrieved from research by Karunarathne et al. [44]. Density correlations was performed with Eq (3.1) and (3.4).

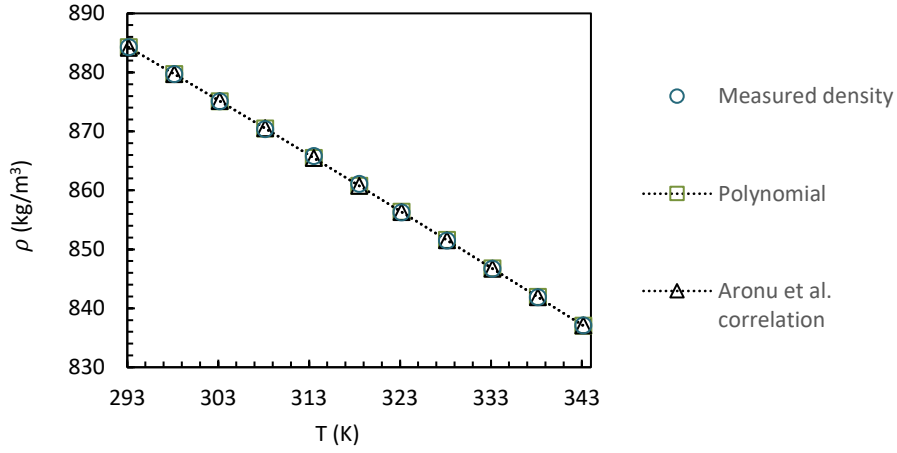| Polynomial		Aronu et al. correlation	
A	1038.79	k_1	382.38
B	-0.21	k_2	0
C	-0.00106	k_3	20425.89
		k_4	416.33
		k_5	-70149.03
		x_1	1
		x_2	0
AARD %	0.009	AARD %	0.011
AMD (kg/m^3)	0.197	AMD (kg/m^3)	0.211

Appendix B.4: Density of pure DEEA

Measured data applied to the calculation was retrieved from research by Karunarathne et al. [44]. Density correlations was performed with Eq (3.1) and (3.4).

Polynomial			Aronu et al. correlation		
A	1087.14		k_1	370.92	
B	-0.48		k_2	0	
C	-0.00074		k_3	-122578.99	
			k_4	423.89	
			k_5	72966.68	
			x_1	1	
			x_2	0	
AARD %	0.012		AARD %	0.012	
AMD (kg/m^3)	0.316		AMD (kg/m^3)	0.329	

Appendix C: Viscosity correlations for pure amines

Appendix C.1: Viscosity of pure AMP

Measured data applied to the calculation was retrieved from research by Karunarathne et al. [43]. Viscosity correlations was performed with Eq (5.1), (5.2) and (5.3).
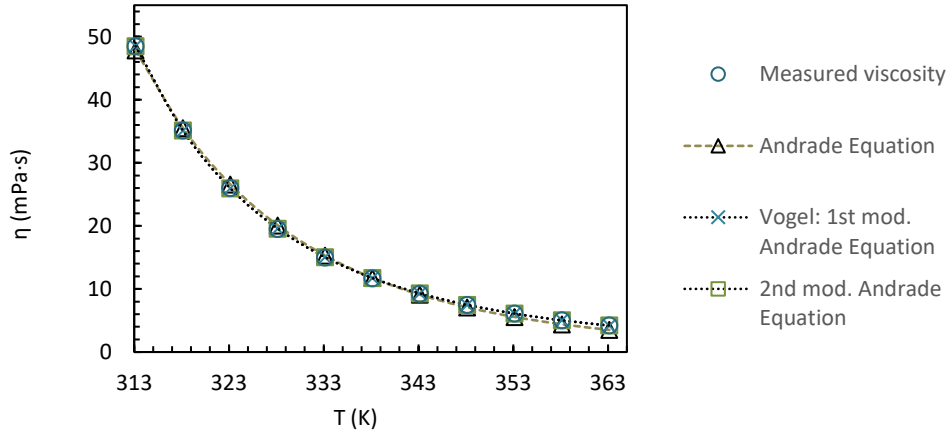

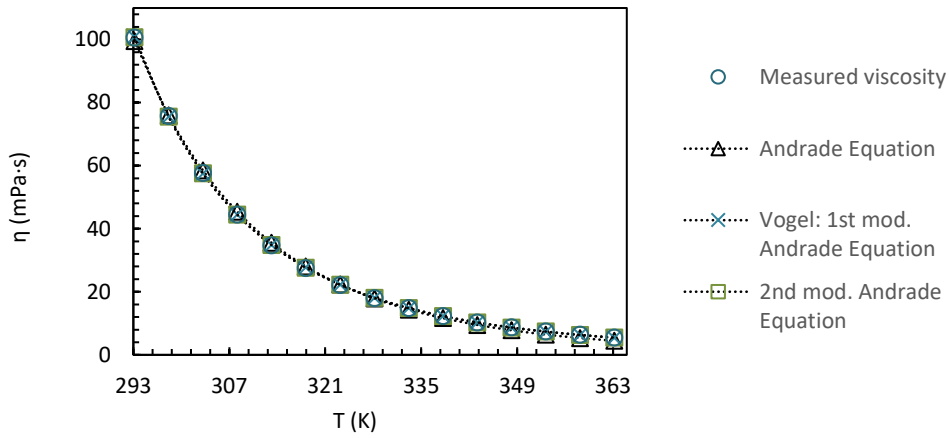| Andrade Equation		Vogel: 1st mod. Andrade Equation		2nd mod. Andrade Equation	
A	-15.13	A	-5.21	A	-7803.30
B	5947.73	B	1230.39	B	2246738.66
		C	-177.86	C	0.00
AARD%	5.080	AARD%	0.395	AARD%	0.184
AMD (kg/m^3)	0.727	AMD (kg/m^3)	0.073	AMD (kg/m^3)	0.045

Appendix C.2: Viscosity of pure MDEA

Measured data applied to the calculation was retrieved from research by Karunarathne et al. [44]. Viscosity correlations was performed with Eq (5.1), (5.2) and (5.3).

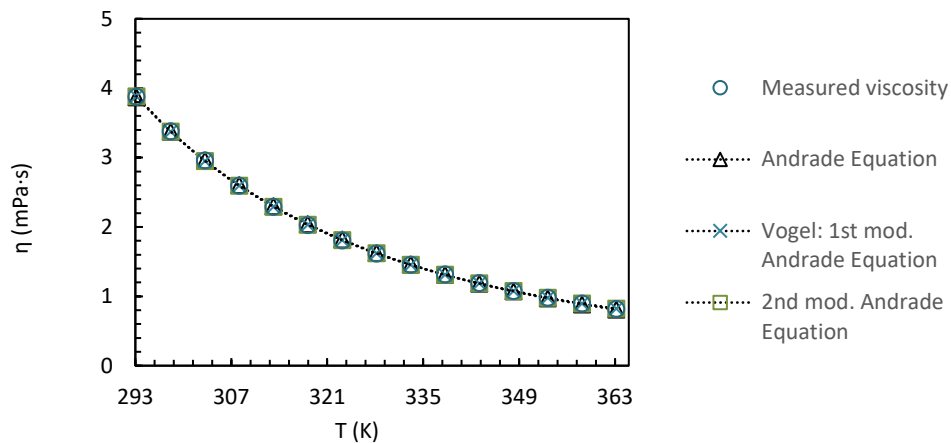| Andrade Equation		Vogel: 1st mod. Andrade Equation		2nd mod. Andrade Equation	
A	-11.51	A	-5.20	A	-1.04
B	4721.82	B	1617.48	B	-1774.08
		C	-128.24	C	1006047.58
AARD%	5.752	AARD%	0.572	AARD%	0.362
AMD (kg/m^3)	1.084	AMD (kg/m^3)	0.252	AMD (kg/m^3)	0.213

Appendix C.3: Viscosity of pure DMEA

Measured data applied to the calculation was retrieved from research by Karunarathne et al. [44]. Viscosity correlations was performed with Eq (5.1), (5.2) and (5.3).

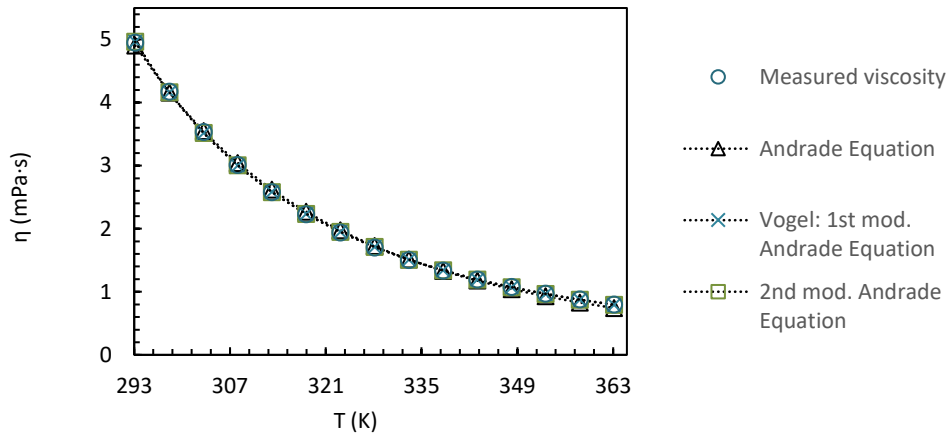| Andrade Equation		Vogel: 1st mod. Andrade Equation		2nd mod. Andrade Equation	
A	-6.78	A	-5.64	A	-5.44
B	2383.10	B	1713.72	B	1530.85
		C	-48.15	C	135077.70
AARD%	0.578	AARD%	0.124	AARD%	0.125
AMD (kg/m^3)	0.014	AMD (kg/m^3)	0.007	AMD (kg/m^3)	0.007

Appendix C.4: Viscosity of pure DEEA

Measured data applied to the calculation was retrieved from research by Karunarathne et al. [44]. Viscosity correlations was performed with Eq (5.1), (5.2) and (5.3).

| Andrade Equation		Vogel: 1st mod. Andrade Equation		2nd mod. Andrade Equation	
A	-8.20	A	-5.02	A	-3.33
B	2870.44	B	1209.94	B	-212.40
		C	-110.43	C	486161.99
AARD%	2.153	AARD%	0.406	AARD%	0.338
AMD (kg/m^3)	0.057	AMD (kg/m^3)	0.015	AMD (kg/m^3)	0.014

Appendix D: Measured data of aqueous MEA

The measured data of Aqueous MEA was found in Karunaratne's research [17]. The tables portray values of the physical properties at a mass ratio (w1) between MEA and water from 0.3 to 1 at temperatures from 293.15 to 363.15K. The mole fraction of MEA is denoted x1.

w1	x1	Measured Density – Aqueous MEA (kg/m^3)							
		293.15K	303.15K	313.15K	323.15K	333.15K	343.15K	353.15K	363.15K
0.3	0.1122	1012.6	1008.2	1003.3	997.9	991.6	986.0	979.4	972.3
0.4	0.1643	1018.4	1013.3	1007.8	1001.8	995.5	988.9	981.9	974.6
0.5	0.2278	1023.6	1017.8	1011.6	1005.2	998.4	991.4	984.1	976.4
0.6	0.3067	1027.7	1021.2	1014.5	1007.6	1000.4	993.0	985.4	977.4
0.7	0.4077	1029.3	1022.4	1015.2	1007.9	1000.4	992.7	984.8	976.4
0.8	0.5412	1028.1	1020.8	1013.3	1005.7	997.9	990.0	981.9	973.6
0.9	0.7264	1023.5	1015.8	1008.1	1000.3	992.4	984.3	976.1	967.8
1	1	1015.9	1008.1	1000.1	992.1	984.0	975.9	967.6	959.3

w1	x1	Measured Viscosity - Aqueous MEA ($mPa \cdot s$)							
		293.15K	303.15K	313.15K	323.15K	333.15K	343.15K	353.15K	363.15K
0.3	0.1122	2.8360	2.1090	1.6280	1.2900	1.0460	0.8660	0.7400	0.6870
0.4	0.1643	4.2850	3.0800	2.3050	1.7820	1.4170	1.1540	0.9600	0.8080
0.5	0.2278	6.6100	4.5800	3.3100	2.4540	1.9150	1.5280	1.2430	1.0290
0.6	0.3067	10.2170	6.7690	4.7360	3.4440	2.6020	2.0310	1.6200	1.3190
0.7	0.4077	15.3480	9.8230	6.6640	4.7200	3.4610	2.6150	2.0290	1.6160
0.8	0.5412	20.5210	12.8400	8.5340	5.9370	4.2950	3.2170	2.4830	1.9620
0.9	0.7264	24.0270	14.9630	9.8790	6.8290	4.9360	3.6830	2.8320	2.2220
1	1	23.3760	14.7480	10.1080	6.9350	5.0670	3.8340	2.9740	2.3640

# Appendix E: Density correlation by Hartono et al. for aqueous MEA

The density correlation, Eq (3.5) and Eq (3.6), of Hartono et al. [16] were tested to compare the method to using the Redlich-Kister polynomial in Chapter 5.3.1. The fit and parameters are shown below. Density information were retrieved from Appendix D, and the data for water were collected from references in Chapter 4.2.
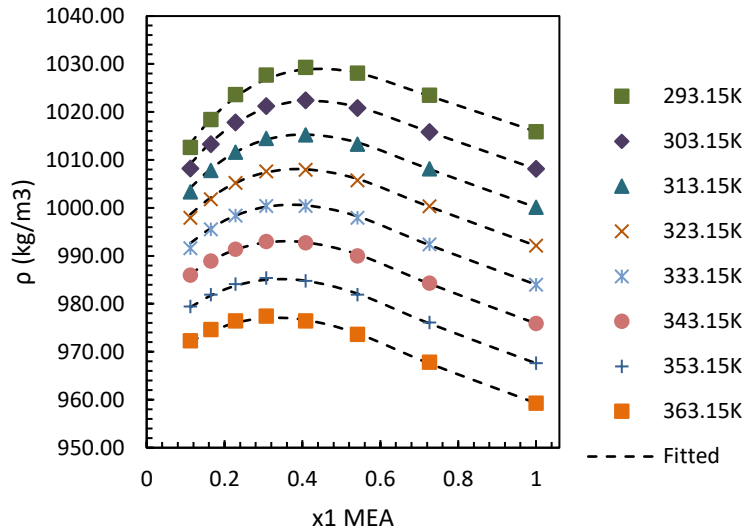
Parameters	
k1	-2.60E-06
k2	2.27E-09
k3	-3.22E-06
k4	3.93E-06
AARD%	0.03
AMD (kg/m^3)	1.06

Appendix F: Viscosity correlation by Bhatt for aqueous MEA

The viscosity relation by Bhatt was computed from Eq (3.55) and (5.6) [34]. The pure viscosity information for MEA were retrieved from Appendix D, while the data for pure water were collected from references in Chapter 4.2.
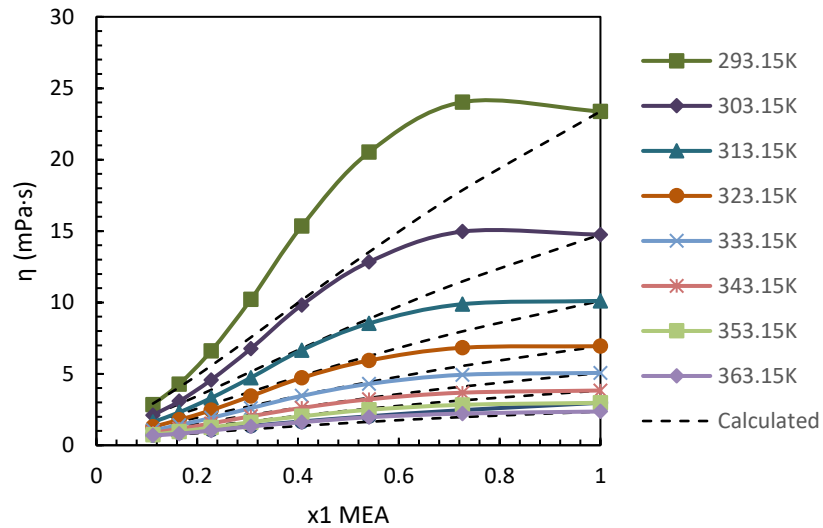
Appendix G: Python 3.6 codes for curve fitting of density data

Appendix G.1: Python 3.6 code – Fitting of density data for pure MEA

```
"""
Code by
Jeanette Larsen (160441@usn.no)
University of South-Eastern Norway,
24.01.21
"""
# Import of packages:
import numpy as np
from scipy.optimize import curve_fit


# T = Temperature, d = Measured density
T = [293.15, 298.15, 303.15, 308.15, 313.15, 318.5, 323.15, 328.15, 333.15, 338.15, 343.15]
d = [884.3, 879.7, 875.1, 870.4, 865.8, 861.1, 856.3, 851.5, 846.7, 841.9, 837.1]


print(d)


# Functions to be curvefitted
def polynomial(T, A, B, C):
    return A+(np.multiply(B,T))+(C*(np.multiply(T,T)))


def aronu_et_al_correlation(T, A, B, C, D, E):
    x_1 = 1
    x_2 = 0
    return
(A+np.multiply(B,x_2)/T)*np.exp(C/np.multiply(T,T)+np.multiply(D,x_1)/T+E*(np.multiply(x_1,x_1)/np.multiply(T,T)))


popt1, pcov1 = curve_fit(polynomial, T, d)
popt2, pcov2 = curve_fit(aronu_et_al_correlation, T, d)


# Displays explanatory text
```

```python
print()
print('Curve fitting for pure MEA density data')
print()
print('Polynomial equation": A+(B*T)+(C*(T**2)), has variables A, B and C =',popt1)
print()
#print(Variance of parameter estimate)
#print(pcov1)
print()
print()
print('Aronu et al. correlation equation: (A+ (B*x_2)/T) * exp(C/(T**2)+ (D*x_1)/T +
E*((x_1**2)/(T**2)))')
print('has variables A, B, C, D and E =', popt2)
print()


# Plotting graph of all functions and measured values
import matplotlib.pyplot as plt
plt.figure(1, figsize=(10,15))
plt.subplot(211)
plt.plot(T, d, 'ro', label = "Measured density data")
plt.plot(T, polynomial(T, *popt1), 'b', label = "Polynomial: A+(B*T)+(C*(T**2))")
plt.plot(T, aronu_et_al_correlation(T, *popt2), 'g', label ="Aronu et al. correlation: (A+
(B*x_2)/T) * exp(C/(T**2)+ (D*x_1)/T + E*((x_1**2)/(T**2)))")
plt.title('curve fitting of density data - pure MEA')
plt.legend( loc='upper right')
plt.show()
```

Appendix G.2: Python 3.6 code – Fitting of density data for aqueous MEA

```python
"""
Code by
Finn Aakre Haugen (Finn.Haugen@usn.no)
University of South-Eastern Norway,
24.02.21
"""
# %% Imports:

import numpy as np
import scipy.optimize
import matplotlib.pyplot as plt


# %% Objective function:

def fun_d(params, x1, T):

    A = params[0]
    B = params[1]
    C = params[2]
    D = params[3]
    E = params[4]

    d = (A + B*(1-x1)/T)*np.exp(C/T**2+ D*x1/T + E*(x1/T)**2)

    return d



def fun_objective(params):

    e_2Darray = np.zeros([len(x1_array), len(T_array)])

    for k_x1 in range(0, len(x1_array)):
```

```python
    for k_T in range(0, len(T_array)):


        x1 = x1_array[k_x1]
        T = T_array[k_T]
        d_pred = fun_d(params, x1, T)
        e_2Darray[k_x1, k_T] = d_obs_2Darray[k_x1, k_T] - d_pred


    sspe = np.sum(e_2Darray*e_2Darray)


    return sspe



# %% Data:


x1_array = np.array([0.1122, 0.1643, 0.2278, 0.3067,
            0.4077, 0.5412, 0.7264])


T_array = np.array([293.15, 303.15, 313.15, 323.15, 333.15,
            343.15, 353.15, 363.15])


d1 = [1012.6, 1008.2, 1003.3, 997.9, 991.6, 986.0, 979.4, 972.3]
d2 = [1018.4, 1013.3, 1007.8, 1001.8, 995.5, 988.9, 981.9, 974.6]
d3 = [1023.6, 1017.8, 1011.6, 1005.2, 998.4, 991.4, 984.1, 976.4]
d4 = [1027.7, 1021.2, 1014.5, 1007.6, 1000.4, 993.0, 985.4, 977.4]
d5 = [1029.3, 1022.4, 1015.2, 1007.9, 1000.4, 992.7, 984.8, 976.4]
d6 = [1028.1, 1020.8, 1013.3, 1005.7, 997.9, 990.0, 981.9, 973.6]
d7 = [1023.5, 1015.8, 1008.1, 1000.3, 992.4, 984.3, 976.1, 967.8]


d_obs_2Darray = np.array([d1, d2, d3, d4, d5, d6, d7])


# %% Guessed values (initial values) of optim variables:


A_guess = 1000
B_guess = 150000
C_guess = -30000
```

```python
D_guess = 600
E_guess = 800


params_guess = np.array([A_guess, B_guess, C_guess,
                D_guess, E_guess])


# %% Solving optim problem:


res = scipy.optimize.minimize(fun_objective,
                params_guess,
                method = 'nelder-mead',
        options = {'ftol': 1e-9, 'disp': True})


# %% Result of optimization:


params_estim = res.x
A_estim = params_estim[0]
B_estim = params_estim[1]
C_estim = params_estim[2]
D_estim = params_estim[3]
E_estim = params_estim[4]
sspe_optim = res.fun


# %% Displaying the optimal solution:
print('Optimal estimates:')
print('A_estim =', f'{A_estim:.3e}')
print('B_estim =', f'{B_estim:.3e}')
print('C_estim =', f'{C_estim:.3e}')
print('D_estim =', f'{D_estim:.3e}')
print('E_estim =', f'{E_estim:.3e}')
print('sspe_optim =', f'{sspe_optim:.3e}')


# %% Plotting:


i = 0  #  Index of temperature array
```

```python
T = T_array[i]
d_pred_1Darray = fun_d(params_estim, x1_array, T)


plt.close('all')
plt.figure(1)


plt.plot(x1_array, d_pred_1Darray, 'bo-',
      label='d predicted at T = ' f"{T}" ' K')
plt.plot(x1_array, d_obs_2Darray[:,i], 'ro',
      label='d observed at T = ' f"{T}" ' K')


plt.title('curve fitting of density data - aqueous MEA')
plt.xlabel('xMEA')
plt.ylabel('Density, d (kg/m^3)')
plt.legend(loc='best')
plt.grid()
# plt.savefig('density.pdf')  # Or: png, jpg, svg.
plt.show()
```